Remote-sensing
Ocean color
Reflectance model
Phytoplankton
Aerosol

Télédétection
Couleur de la Mer
Modèle de réflectance,
Phytoplancton
Aérosols

Atmospheric corrections and interpretation of marine radiances in CZCS imagery, revisited

Jean-Michel ANDRÉ, André MOREL

Laboratoire de Physique et Chimie marines, La Darse, BP 08, 06230 Villefranche-sur-Mer, France.

Received 29/03/90, in revised form 24/07/90, accepted 31/07/90

ABSTRACT

In a previous study (Bricaud and Morel, *Oceanologica Acta*, 1987), a reflectance model developed for oceanic Case 1 waters was introduced into CZCS data processing, mainly with the aim of improving the atmospheric correction scheme and permitting discrimination between Case 1 and turbid Case 2 waters. The present paper, not limited to CZCS, examines the possible extension of the use of this reflectance model. In particular, it is proposed that the relationships required in iterative computations when estimating marine radiances in the four (visible) channels be those which derive from the model rather than the empirical expressions. Also, in order to ensure an internal coherency, it is proposed to operate the modelled relationships between the reflectance ratios and the chlorophyllous pigment concentration as algorithms for pigment retrieval. The performances of a pixel-by-pixel procedure (PPP), which iteratively produces the best estimates of both the atmospheric and the marine signals, are assessed through sensitivity analyses. To this end, the application of PPP (or any other procedure) is simulated by using a modelled ocean-atmosphere system, in which the aerosol properties, the pigment content, the sun and viewing geometrical conditions can be changed. We also examine the consequences:

- of using a mean Angström exponent instead of those which result at the pixel level from the application of the PPP;
- of considering the "full" pigment concentration range when applying the PPP, *i.e.* a range which considerably exceeds that of "clear water";
- of the inevitable deviation of actual waters with regard to the modelled Case 1 waters (which are underlying as reference waters in such a processing). It is believed that improvements can be expected from the present procedure, with the proviso that well calibrated, remotely sensed data should be available.

Oceanologica Acta, 1991. **14**, 1, 3-22.

RÉSUMÉ

Corrections atmosphériques et interprétation des luminances marines dans l'imagerie CZCS

Dans une étude précédente (Bricaud et Morel, *Oceanologica Acta*, 1987), un modèle de réflectance développé pour les eaux de mer du cas 1 et introduit dans l'algorithmique de traitement des données CZCS avait pour but d'améliorer les corrections atmosphériques et de rendre possible une discrimination des eaux des cas 1 et 2. La présente étude, qui ne concerne pas le seul CZCS, examine la possibilité d'une extension à l'utilisation de ce modèle. Il est en particulier proposé de remplacer les relations empiriques utilisées dans les (inévitables) procédures itératives, lesquelles relient entre elles les luminances marines dans les quatre canaux visibles, par des relations dérivées elles aussi du modèle de

réflectance. Dans le but d'assurer une cohérence interne à la méthode, il est proposé d'utiliser également le modèle pour l'estimation des concentrations en pigments chlorophylliens à partir des rapports de réflectances. Les performances d'une procédure de correction itérative, capable d'opérer pixel par pixel la meilleure estimation des signaux marins et aérosols, sont étudiées dans le cadre d'une analyse de sensibilité. Dans ce but, l'application de cette procédure, baptisée PPP, est simulée en utilisant un modèle optique couplant l'océan et l'atmosphère dans lequel il est possible de faire varier les propriétés des aérosols, la concentration en pigments, et les géométries du soleil et de la visée. Sont également examinées :

- les conséquences de l'utilisation d'une valeur moyenne de l'exposant d'Angström de l'aérosol au lieu des valeurs que la PPP est capable d'évaluer à chaque pixel ;
- le comportement de la PPP lorsqu'on la confronte à la gamme complète des valeurs possibles du contenu de l'océan en phytoplancton, gamme qui excède largement celle des "eaux claires" ;
- la réponse de la PPP aux déviations que présentent naturellement les eaux de mer par rapport à des eaux du cas 1 en conformité avec les prédictions du modèle. Des progrès peuvent être attendus de l'emploi de cette procédure dans la mesure où les mesures spatiales auxquelles l'appliquer sont, ou seront, radiométriquement bien calibrées.

Oceanologica Acta, 1991. **14**, 1, 3-22.

A work with this title was presented by A. Bricaud and A. Morel at the Symposium on"Spatial Oceanography", held in Brest (France) in November 1985 and published in a special issue of *Oceanologica Acta* (1987), available in the course of 1988. Since the submission of that paper (in April 1986), some progress has been made, some hidden problems have been identified, and alternative solutions have been explored. It seems timely to present the latest developments in the processing of the (defunct) Coastal Zone Color Scanner (CZCS) data, to the extent that, besides a need for an optimized use of the archived data, open questions remain that are common to CZCS and future sensors. The present study deals only with Case 1 waters, *i.e.* waters for which phytoplankton and their associated by-products (debris, heterotrophic bacteria, dissolved yellow organic matter) control the optical properties. The question of discriminating between these waters and the turbid Case 2 waters, examined in detail by Bricaud and Morel (1987), is not reconsidered here.

The topics dealt with in the present study, remain essentially the same as in Bricaud and Morel (1987). Therefore, in order to avoid duplication of previously published material, we limit ourselves to a brief summary of the CZCS data correction scheme and refer the reader to the earlier paper (thereafter called BM) for a detailed description. The symbols and definitions used in BM are kept unchanged and, in particular, the equations quoted in the present paper by arabic numbers are those appearing with an identical number in BM (for convenience they are reproduced in the present Tab. I), while the new ones introduced are numbered with roman numbers.

Problems induced by uncertainties in the CZCS sensor calibration and by sensitivity degradation are beyond the scope of the present paper. It is acknowledged, however, that these instrumental deficiencies are, in practice, at the origin of major difficulties when processing the data, so that improvements will remain illusory as long as scenes with reasonably well-calibrated signals are not considered.

INTRODUCTORY ANALYSIS

The basic problem of the ocean remote sensing in the visible part of the spectrum

The radiances measured at visible wavelengths by a spaceborne sensor directed at the ocean originate mainly (typically 90 %) from the scattering of solar radiation by molecules and aerosol particles within the atmosphere, L_R and L_A respectively. This considerable atmospheric signal has to be accurately estimated in order to extract properly0 the remaining part of the signal, *i.e.* the "marine signal", L_W, which carries information about the water content, essentially concerning the algal biomass in Case 1 waters. This information is interpreted in terms of pigment concentration (chlorophyll *a* + pheophytin *a*, in $mg.m^{-3}$) within the upper layer of the ocean, through the use of "marine algorithms".

The calculation of the molecular part of the atmospheric signal is easily effected, the only required quantity being the ground pressure. As regards radiance due to aerosol, a separate estimate would require the knowledge of its integrated concentration and its spectral scattering properties (conveniently described by the so-called Angström exponent, denoted *n*). In visible remote sensing of the ocean (in particular when using CZCS), no *a priori* or independently acquired information concerning aerosol is available. Therefore the marine and aerosol signals have to be simultaneously extracted from the total signal recorded by the remote sensor, and the missing information must be replaced by external

Table 1

Equations reproduced from Bricaud and Morel (1987), for use in the present study.
Équations reproduites de Bricaud et Morel (1987), pour les besoins de la présente étude.

$L_T(\lambda, \theta, \theta_o, \phi) = L_R(\lambda, \theta, \theta o, \phi) + L_A(\lambda, \theta, \theta o, \phi) + t((\lambda, \theta) L_W(\lambda, \theta, \theta o)$	(4)
$L_A(\lambda, \theta, \theta_o, \phi) = F'_o(\lambda) \tau_A(\lambda) \omega_A(\lambda) p_A(\lambda, \theta, \theta_o) / 4 \pi \cos\theta$	(5')
$F'_o(\lambda) = F_o(\lambda) \exp[-\tau_{O_3}(\lambda) (1/\cos\theta + 1/\cos\theta_o)]$	(6)*
$p_A(\lambda, \theta, \theta_o) = P_A(\lambda, \gamma-) + [\rho(\theta, \lambda) + \rho(\theta_o, \lambda)] P_A(\lambda, \gamma+)]$	(7)*
$\cos\alpha \pm = \pm \cos\theta \cos\theta_o - \sin\theta \sin\theta_o \sin\phi$	(7')*
$t(\lambda, \theta) = \exp\{-[0.5 \tau_3(\lambda) + \tau_{O_3}(\lambda)] / \cos\theta\}$	(8)
$R(443)/R(670) = 5.98 [R(443)/R(550)]^{1.47}$	(10 *a*)
$L_W(\lambda) = \{[1-\rho(\theta, \lambda)] (1-\bar{\rho}) \cos\theta_o F_o(\lambda) t(\theta_o, \lambda)/Q\ m^2(\lambda)\} R(\lambda)$	(14)
$C = 1.73 [R(443)/R(550)]^{-2.04}$	(15 *a*)
$C = 2.51 [R(520)/R(550)]^{-6.38}$	(15 *b*)

Definitions

T, W, A, R, O_3	: (as subscripts) correspond to: total, marine, aerosol, Rayleigh and absorbing gazes (mainly ozone), respectively
L	: radiance
λ	: wavelength
θ	: zenith angle of sighting direction (pixel to spacecraft)
θ_o	: Sun zenith angle (pixel to Sun)
ϕ	: azimuth angle difference between the vertical planes containing sensor and Sun
τ	: optical thickness
ω	: single scattering albedo
F_o	: extraterrestrial solar irradiance
P	: scattering phase function
ρ	: Fresnel reflectance coefficient of the air-sea interface
t	: diffuse transmittance of the atmosphere
$\bar{\rho}$	: Fresnel coefficient of the sea surface averaged over all angles (set equal to 0.04)
Q	: underwater irradiance-to-radiance ratio (set equal to 4.5)
m	: seawater refractive index
R	: reflectance at null depth

* A few typographical errors occurred in these equations in Bricaud and Morel (1987), which are corrected in the present table.

constraints to solve the problem. Ocean reflectance models, combined with empirical relationships by which the water-leaving radiances, $L_W(\lambda)$, in the various spectral channels are interlinked , provide such constraints. Their introduction into the data processing generally results in iterative computational schemes, which finally permit decoupling of the marine and aerosol signals, in the four visible channels of CZCS (λ_1 = 443, λ_2 = 520, λ_3 = 550 and λ_4 = 670 nm).

Present available solutions

Such CZCS correction schemes have been developed (Gordon *et al.*, 1983; Bricaud and Morel, 1987). The principle is, in a first phase of the processing, to select some pixels for which external information (reasonable hypotheses, modelled reflectance values) about the marine optical properties exist and can be introduced. After the marine signals are estimated for these pixels, the aerosol signals, $L_A(\lambda)$, can be computed in different channels, and the Angström exponent *n* is derived. For Gordon *et al.* (1983), such pixels are those with a chlorophyllous pigment concentration lower than 0.25 $mg.m^{-3}$ ("clear water" pixels). In this case, their "normalized radiances", *i.e.* the radiances they would backscatter toward the zenith in the absence of atmosphere in channels 2, 3 and 4 are assumed to be known and constant (Gordon and Clark, 1981). For Bricaud and Morel (1987), these pixels may contain up to 1 or 2 $mg.m^{-3}$ and their marine signals, no longer constant, can still be evaluated in all channels, as a function of their pigment concentration, by using a reflectance model (Morel, 1983 and 1988), combined with an iterative computation scheme. Such a combination is also proposed by Gordon *et al.* (1988), and relies on their radiance model.

For the pixel selection, a kind of pre-processing is effected which excludes a variable, sometimes considerable, number of pixels. The methods which make use of reflectance models (and can cope with a wider pigment range) are less stringent than those which retain only the "clear water" pixels. In any case, the atmospheric correction remains to be done for those pixels previously left out. It makes use of Angström exponent values extrapolated from regions where it was possible to extract them (see below, "residual problems"). For these pixels also, however, the resort to an iterative process remains necessary in order to estimate the aerosol contributions (at least in one channel). The iterative scheme, originally proposed by Smith and Wilson (1981), is based on an empirical relationship between the water-leaving radiances at three wavelengths (*see* also discussion and Figure 2 in BM). This statistical relationship, derived from a linear

regression analysis using the log transform of *in situ* data, is:

$$L_w(443)/L_w(670) = 12.06\ [\ L_w(443)/L_w(550)\ ]^{1.66}$$

$L_w(\lambda)$ being related to $R(\lambda)$, the diffuse reflectance of the ocean just below the surface, (according to equation 14, Table), a more general formulation of the above relationship is:

$$r_{1,4} = A\,(r_{1,3})^B \qquad (I)$$

where $r_{i,j} = R(\lambda_i)/R(\lambda_j)$.
By using such a relationship, the marine and aerosol radiances can be iteratively partitioned.

As regards the estimate of the pigment concentration from the water-leaving radiances, this is generally carried out by operating empirical algorithms (also of statistical nature), the form of which is:

$$C = D\,(r_{i,j})^E \qquad (II)$$

where C is the pigment concentration (in $mg.m^{-3}$), and i = 1 or 2, and j = 3 (the factor and exponent, D and E, like A and B in equation I, result from regression analyses of the field data).

Residual problems, inconsistencies and possible remedies

ALGORITHMS AND ITERATION

As seen above, the estimate of the aerosol scattering spectral dependency is achieved owing to a marine reflectance model. Its use, however, is intermingled with the use of empirical relationships, namely the marine algorithms I and II above. There is an obvious lack of internal coherency in such a mixing mode.

Moreover, it is generally admitted that the ratio $r_{1,3}$ [in equation (II)] is no longer usable when attempting to retrieve "high" pigment concentrations (more than 1-2 $mg.m^{-3}$), and that it must be replaced by $r_{2,3}$. The reason is that the blue radiance emerging from the ocean, $L_w(443)$, decreases when the pigment concentration increases, in such a way that it may become insignificant (in terms of digital counts). Thus, if $L_w(443)$ is considered as not reliable when computing the pigment content, the logical consequence is simultaneously to abandon equation (I) which involves this signal. The iteration scheme which depends on the use of this equation fails, if not modified. The modification (in effect the generalization of the method) which can be imagined consists of developing a similar relationship, except that it involves L_w in channels 2, 3 and 4 (instead of 1, 3 and 4).

Another source of inconsistency lies within the switching procedure itself, from $r_{1,3}$ to $r_{2,3}$, as evoked above. The empirical algorithms [equation (II)] involving either $r_{1,3}$ or $r_{2,3}$ are, because of their statistical nature, not perfectly compatible. The help of the reflectance model to remove this numerical incompatibility, as well as to improve and extend the capability of the iterative method is a possible issue, which must be analysed. This is the first aim of the present paper.

EXTRAPOLATION OF AEROSOL PARAMETERS

From selected pixels (Case 1 waters with concentration less than a certain upper limit value), individual n-values are obtained. Before extrapolating to regions where n was not accessible, a common practice is to average these n-values over a more or less arbitrary number of pixels and use this mean value elsewhere. In fact, from one pixel to another, individual n values exhibit some dispersion and differ from the mean value. This is due to :

- natural variations in the aerosol population (marine, continental or crustal origin, influence of humidity...) which are spatially organized, with scales and structures typical of the atmospheric motions;
- artifactual reasons, added to the natural variability. In effect, the estimate of the aerosol exponent, where this is possible, remains inevitably imperfect, relying on assumptions concerning the radiative transfer in the atmosphere and in the ocean (namely: that the aerosol does not absorb; that its phase function does not depend upon the wavelength; that the coupling term between aerosol and molecular scattering is negligible; that Case 1 waters obey the reflectance model; that the underwater irradiance-to-radiance ratio is constant and given a "reasonable" value; and that Fresnel reflections occur on the flat surface of a calm ocean ...). These assumptions are known to render more or less erroneous the computed exponent. An important character of these misestimates is that they vary spatially with the geometrical configuration of the remote sensing, along a scan line, for instance.

For both the above reasons, the mean n value extended to the rest of the image or to the whole scene may significantly depart from the local "actual" values. This is expected to have an impact on the quality of the pigment concentration retrieval. To examine this impact is the second aim of the present work. A simulation is effected by allowing local, supposedly true, n values to differ from the mean value, whereas pigments will be computed by following the "standard" method operated with the adopted mean n value.

The procedure described in Bricaud and Morel (1987), and that suggested in Gordon *et al.* (1988) have, in fact, the capacity of correcting for the aerosol effect on a pixel-by-pixel basis regardless of the pigment concentration, at least below a reasonable limit, admittedly about 2 $mg.m^{-3}$ or perhaps more. The drawbacks induced by the use of a mean Angström exponent, in principle, would cancel out. The results of such a pixel-by-pixel procedure (PPP), however, did not prove to be fully efficient (*see* discussion in BM), in the sense that pigment and aerosol exponent maps (simultaneously produced) still showed some residual correlations, especially in zones with relatively high pigment concentration (>1.5 $mg.m^{-3}$).

Therefore the real potentiality of the PPP is firstly re-examined by simulating remote sensing situations with an "ideal" ocean (which rigorously obeys the optical reflectance model), and with a variable aerosol load and nature. The PPP is in principle fully efficient, thus the (ideal) marine signals must be retrieved at the issue of the processing, whatever the aerosol and the remote sensing geometry. This, however, remains to be verified.

Natural oceans, however, differ from this ideal ocean. Thus, a characteristic and perhaps underlying pitfall of such a pixel-by-pixel procedure is that the large use made of the reflectance model obviously tends to force the optical properties, as retrieved for the ocean, to conform strictly to those predicted by the model. Due to the natural variability within the Case 1 waters, some deviations are expected to occur between the true and the modelled reflectances. Studying the importance of these departures and the way the PPP can cope with this variability is the third aim of the present study.

The organization of the paper is as follows. An overview of the numerical aspects of the CZCS data processing is given first for the sake of self-consistency (more details are to be found in BM), and improvements of the marine algorithms are proposed. The general scheme for simulating the ocean-atmosphere system is then presented. This modelled system is used to examine the danger related to the extrapolation of the aerosol properties, namely the Angström exponent. Finally the efficiency of the pixel-by-pixel procedure is analysed also by using the ocean-atmosphere model.

AVAILABLE PROCEDURES AND PROPOSED MODIFICATIONS

Summary of the procedures

As developed in Bricaud and Morel, CZCS data processing comprises two intermeshed iterative computations, in what follows termed BMP1 and BMP2.

BMP1 allows the marine signals to be extracted from CZCS data when the Angström exponent is assigned a fixed value (*see* Fig. 1 *a*). Briefly, algorithm 10 *a* (*see* Table 1), which relates $r_{1,3}$ and $r_{1,4}$, provides successive re-estimates of the reflectance in the red, R(670), as a function of those in the blue, R(443), and in the green, R(550), (according to BM; i could only be 1 in Fig. 1 *a*). Once the convergence is achieved, the pigment

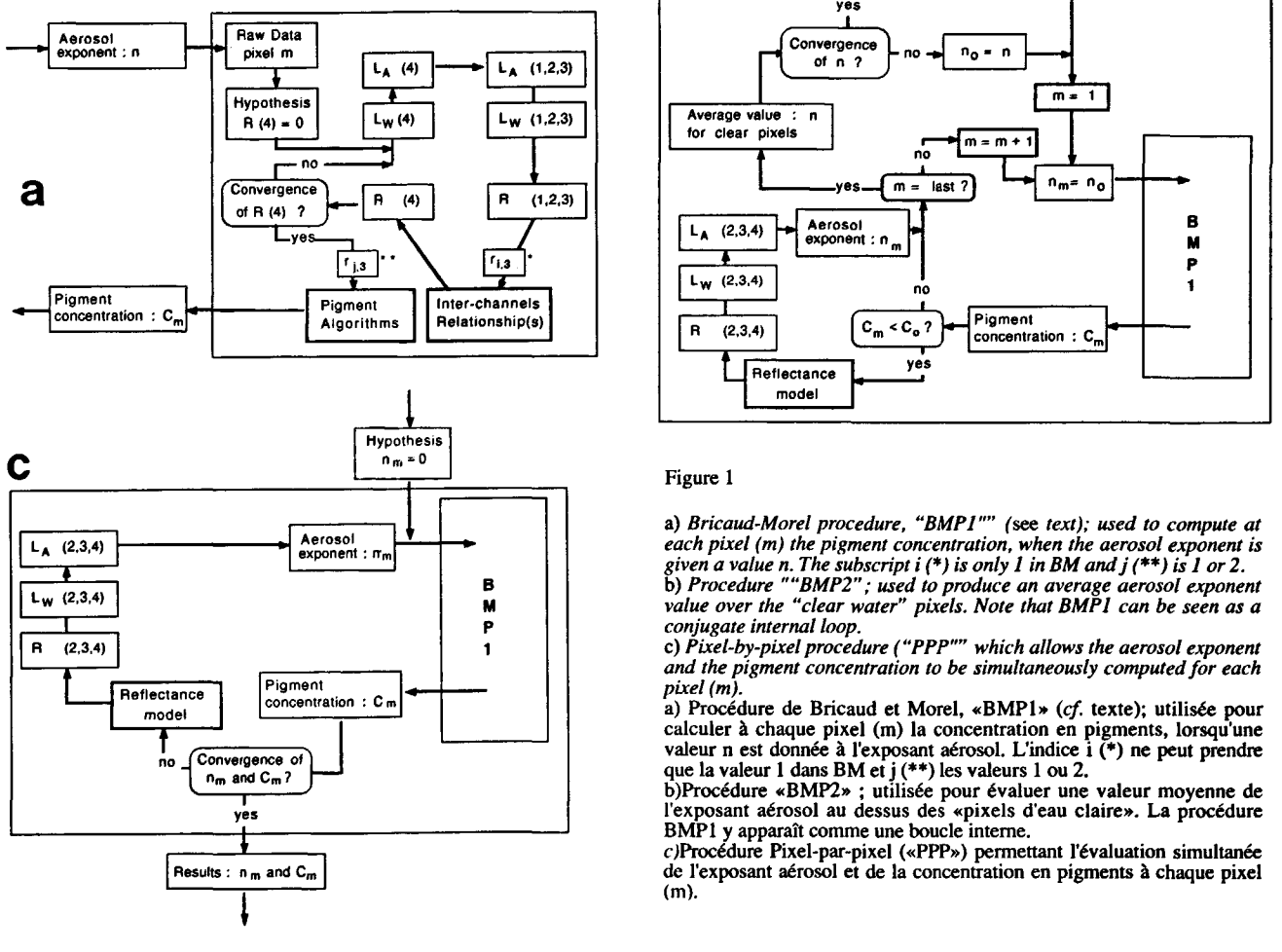

Figure 1

a) *Bricaud-Morel procedure, "BMP1"" (see text); used to compute at each pixel (m) the pigment concentration, when the aerosol exponent is given a value n. The subscript i (*) is only 1 in BM and j (**) is 1 or 2.*
b) *Procedure ""BMP2"; used to produce an average aerosol exponent value over the "clear water" pixels. Note that BMP1 can be seen as a conjugate internal loop.*
c) *Pixel-by-pixel procedure ("PPP"" which allows the aerosol exponent and the pigment concentration to be simultaneously computed for each pixel (m).*
a) Procédure de Bricaud et Morel, «BMP1» (*cf.* texte); utilisée pour calculer à chaque pixel (m) la concentration en pigments, lorsqu'une valeur n est donnée à l'exposant aérosol. L'indice i (*) ne peut prendre que la valeur 1 dans BM et j (**) les valeurs 1 ou 2.
b)Procédure «BMP2» ; utilisée pour évaluer une valeur moyenne de l'exposant aérosol au dessus des «pixels d'eau claire». La procédure BMP1 y apparaît comme une boucle interne.
c)Procédure Pixel-par-pixel («PPP») permettant l'évaluation simultanée de l'exposant aérosol et de la concentration en pigments à chaque pixel (m).

concentration in Case 1 waters is derived from the blue-to-green reflectance ratio $r_{1,3}$ by using the pigment algorithm 15 *a*, or alternatively from the blue-green-to-green ratio $r_{2,3}$ by using the algorithm 15 *b* (according to BM; *j* is either 1 or 2 in Fig. 1 *a*).

The above computation is, in effect, an internal loop inside BMP2, the aim of which is to evaluate a mean value of the Angström exponent over all the "clear water" pixels present within the (sub) scene processed. BMP2 is represented in Figure 1 *b*. Using a first guessed value for the exponent (n_o = 0, in general), BMP1 provides a first estimate of the pigment content, C_m, at each pixel m. For the pixels containing less than a limit value C_o (Bricaud and Morel decided that C_o = 1.5 $mg.m^{-3}$ was a reasonable limit), the Case 1 reflectance model provides, as a function of C_m, a re-estimate of the marine reflectances in channels 2, 3 and 4. This allows the re-evaluation of the corresponding aerosol signals, and thence of a "new" exponent value n_m (for each pixel m such that $C_m < C_o$). These individual values,nm, are then averaged, and the resulting mean value, n, is used for a second iterative estimate (BMP1) of the pigment concentration at each pixel, allowing an improved selection of the pixels with $C_m < C_o$, and so on. The successive mean values generally converge toward a limiting value which will be used, in a last run of BMP1, to obtain the final pigments estimate for all the (Case 1) pixels within the (sub) scene processed (this final step of the entire processing is not represented in Fig. 1 *b*).

Another combination of the same procedures, also possible, allows for each pixel a simultaneous estimate of the aerosol exponent and of the pigment concentration. It is the basis of a pixel-by-pixel procedure (PPP), and the corresponding scheme is shown in Figure 1 *c*. Its specificity is that the iterative estimate of the exponent is pursued, till convergence, at each pixel, regardless of its pigment content. This procedure, attempted by Bricaud and Morel, produced the pigment content and aerosol maps of their Figures 6 and 15 *b*.

Modifications: reflectance-model-based against empirical algorithms

The lack of coherency resulting from the combined use of empirical and modelled relationships in the BM procedures is examined and improvements are proposed. Are of concern:

- the manner for inter-relating the marine signals at various wavelengths (which is the tool for an iterative estimate of R (670);
- the algorithms to be used to derive the pigment concentration.

Interrelating the marine signals at various wavelengths

In Figure 2, we compare the empirical relationship linking $r_{1,3}$ and $r_{1,4}$ (equation 10 *a*, *see* Table 1), with the equivalent relationship derived from the reflectance model. As shown, the empirical curve (dotted line) and the modelled curve (continuous line) are in rather good agreement, albeit with slight differences:

- at both ends of the $r_{1,3}$ range, the linear regression, by nature, cannot account for the non-linear optical effects which, on the contrary, are integrated in the modelling (*see* Morel, 1988);
- the empirical $r_{1,4}$ values always exceed the modelled values. This excess is mainly due to the inaccurate determination at sea of the reflectance in the red part of the spectrum, because the upwelling flux (in this spectral domain where absorption is high), is very sensitive to the depth of measurement and cannot be easily corrected for (*i.e.* extrapolated to exact null depth). The relationship based on the reflectance model is therefore believed to be

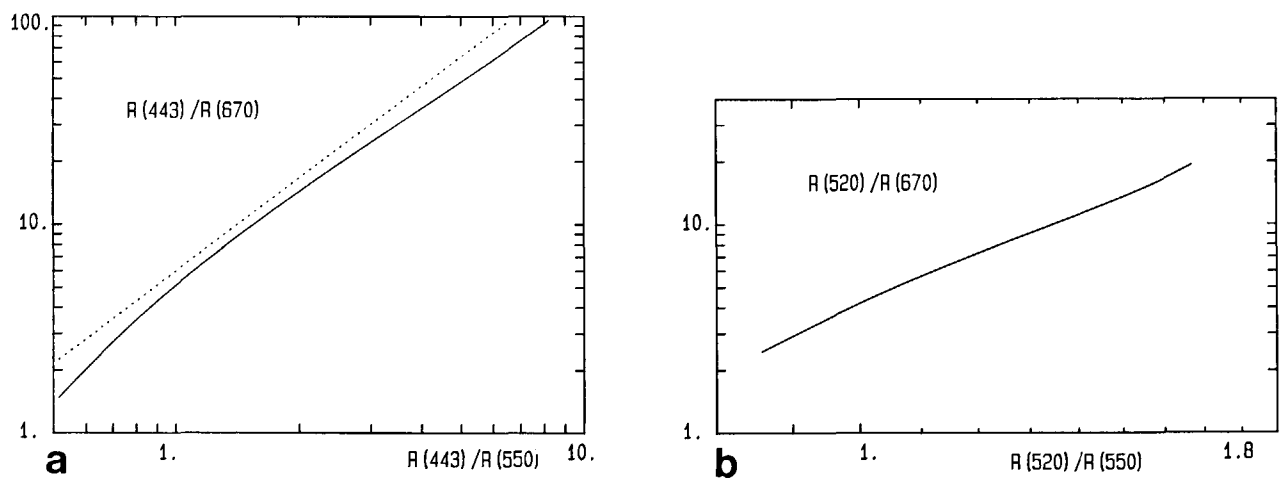

Figure 2

a) *"Blue-to-red" reflectance ratio as a function of the "blue-to-green" reflectance ratio. Solid line: modelled relationship. Dotted line: empirical relationship.*
b) *"Blue-green-to-red" reflectance ratio as a function of the "blue-green-to-green"" reflectance ratio (modelled relationship).*
Rapport «bleu-sur-rouge» des réflectances en fonction du rapport «bleu-sur-vert». Trait continu : relation modélisée. Pointillé : relation empirique.
Rapport«bleu-vert-sur-rouge» des réflectances en fonction du rapport «bleu-vert-sur-vert» (relation modélisée).

more reliable. Note that the model itself depends on a statistical analysis of *in situ* data, including those in the red; the inaccuracy mentioned above is still less penalizing as downwelling flux data, as well as wider depth intervals, are involved in the computation of the attenuation coefficient for downwelling irradiance (from which reflectance is derived).

From the model, and taking into account the spectral response of CZCS channels, the following polynomial fit has been established:

$$\log r_{1,4} = 0.693 + 1.62 (\log r_{1,3}) - 0.265 (\log r_{1,3})^2 \quad \text{(III } a\text{)}$$

The $r_{1,4}$ values produced by this polynomial fit coincide with the exact modelled values within less than 1 % (RMS error). This relationship is henceforth introduced in the CZCS data processing.

As long as the water-leaving radiance at 443 nm can be considered as sufficiently significant, the relationship I (Fig. 2 in BM), and, better, its modelled substitute III a, can be used. As shown in Figure 3, the unreliability threshold (3-4 numerical counts) for the digitized blue signal is crossed when the pigment content exceeds 2-8 $mg.m^{-3}$, depending upon the viewing and lighting conditions. Above 1-2 $mg.m^{-3}$, $L_w(520)$ is significantly higher than $L_w(443)$, and could be used instead, provided that the relationship between $r_{2,3}$ and $r_{2,4}$ is produced. To our knowledge, no empirical relationship similar to Eq. 10 *a* but involving L_w in channels 2,3 and 4, has ever been established. The $r_{2,3}$ ratio, unfortunately, is known to be much less responsive to C than $r_{1,3}$. This fact, added to the inescapable inaccuracy of the $L_w(670)$ measurements, discourages trust in linear regression techniques when applied to *in situ* measurements. For this reason, and also to preserve the overall consistency of the processing, the following expression has been derived from the model:

$$\log r_{2,4} = 0.619 + 3.17 (\log r_{2,3}) - 1.30 (\log r_{2,3})^2 \quad \text{(III b)}$$

(RMS error in the polynomial fit less than 1 %). This relationship, graphically presented in Figure 2 *b*, is also incorporated into the computational process.

With the alternative now offered by the inter-channel relationships III *a* and III *b*, the iterative procedure allowing the partition between marine and aerosol signals (Fig. 3 in BM, and Fig. 1 *a* in this study), can be operated even when the blue signal is vanishing (with equations III *a*, and III *b*, i can now be 1 or 2, in Fig. 1 *a*).

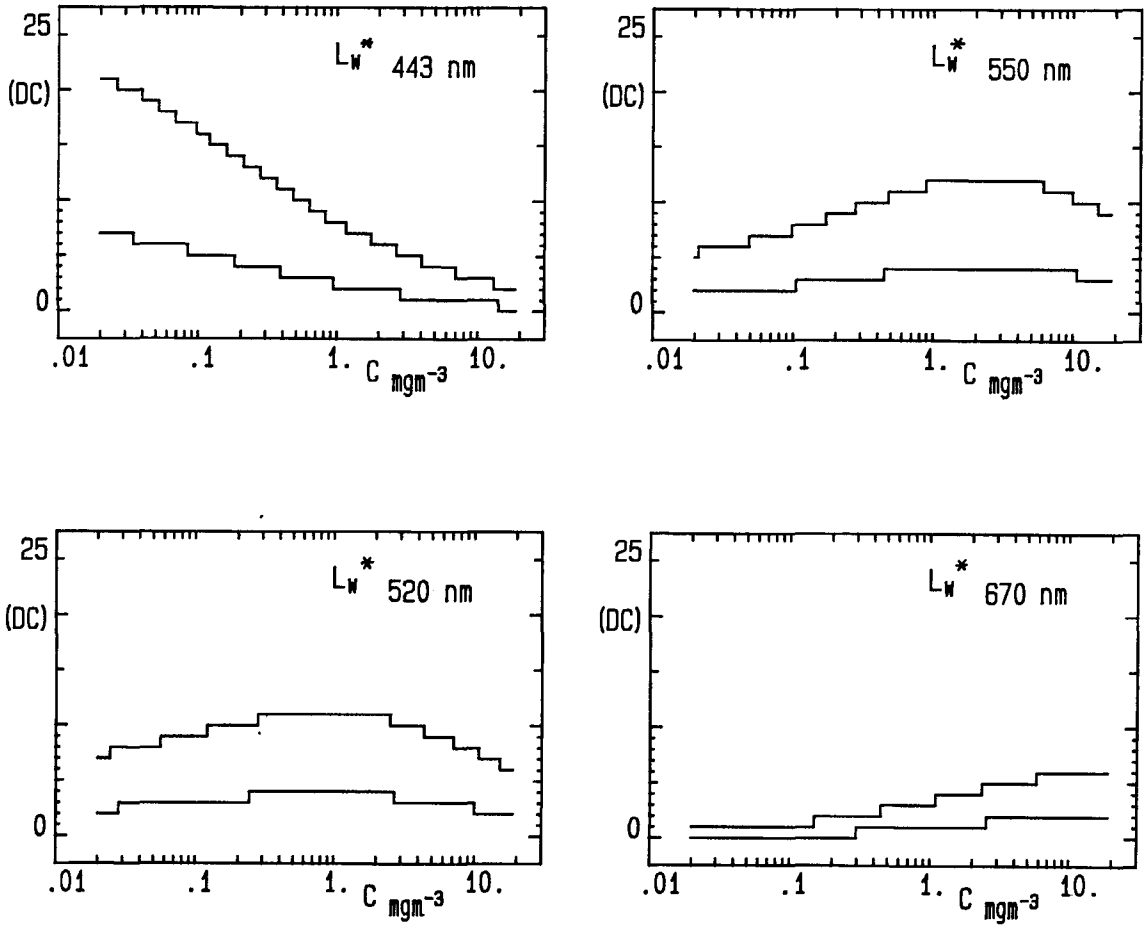

Figure 3

Marine signals at spacecraft level as a function of pigment concentration in CZCS channels 1 to 4. The upper stepped curve in each panel corresponds to $\theta = 20°$ and $\theta_o = 0°$, and the lower one to $\theta = 40°$ and $\theta_o = 65°$.
Signaux marins au niveau du satellite, en fonction de la concentration en pigments, dans les cannaux 1 à 4 de CZCS. Dans chaque panneau la courbe supérieure correspond au couple $\theta = 20°$, $\theta_o = 0°$, et la courbe inférieure au couple $\theta = 40°$, $\theta_o = 65°$.

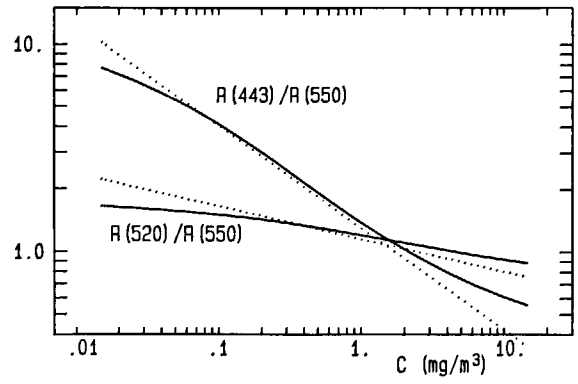

Figure 4

Blue-to-green and blue-green-to-green reflectance ratios as a function of pigment concentration. Solid lines: modelled relationships. Dotted (straight) lines: empirical relationships.
Rapports «bleu-sur-vert» et «bleu-vert-sur-vert» des réflectances en fonction du rapport de la concentration en pigments. Traits continus : relations modélisées. Pointillés : relations (linéaires) empiriques.

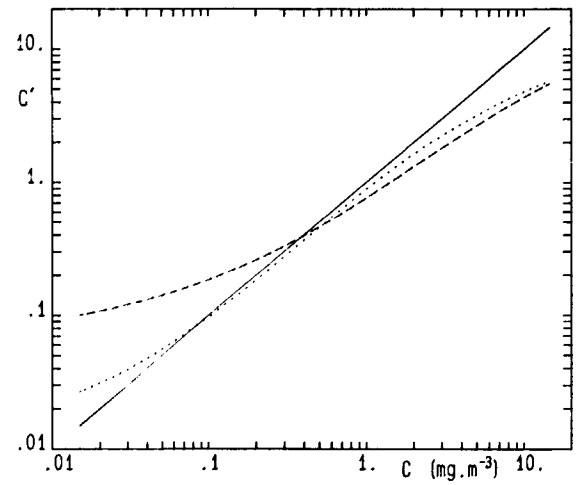

Figure 5

Pigment concentration C' as retrieved by applying the empirical blue-to-green pigment algorithm (dotted line) and the blue-to-green algorithm (dashed line) to Case 1 modelled waters with variable pigment concentration, C. When the modelled pigment algorithms are used, C' and C coincide (solid 1:1 line).
Concentrations en pigments C' obtenues en appliquant l'algorithme empirique «bleu-sur-vert» (en pointillé), et l'algorithme «bleu-vert-sur-vert» (en tireté), à des eaux du cas 1 modélisées, de concentrations en pigments variables, C. Lorsque les algorithmes modélisés sont employés C' et C coïncident (droite en trait continu).

PIGMENT ALGORITHMS

The empirical algorithms used in BM (their Figures 10 *a* and 10 *b*), tailored according to equation II, are shown by the dotted lines in Figure 4, whereas the solid curves represent the ratios of the same spectral reflectances when computed from the model as a function of the pigment concentration C (the spectral profiles of the CZCS channels are taken into account). As already noted in Gordon and Morel (1983, their Fig. 8), the agreement between empirical and modelled relationships, excellent in the middle part of the C range, becomes progressively degraded toward very low and high C values. For such values, the use of empirical algorithms inevitably leads to misestimates. Their magnitude is readily placed in evidence by applying the empirical algorithms to reflectances produced by the model for various C values (Fig. 5). The C' values so obtained are overestimates of C in oligotrophic waters ($C < 0.06$ mg.m^{-3}), or underestimates in meso/eutrophic waters ($C > 2$ mg.m^{-3}). As far as CZCS data are concerned, such underestimates are somewhat hypothetical, to the extent that the sensitivity of the $r_{2,3}$ algorithm, of order for these high concentration waters, is rather poor (see discussion in BM, and in Gordon *et al.* 1988). On the contrary, the $r_{1,3}$ algorithm is very sensitive to small pigment changes in oligotrophic waters, and $L_w(443)$ is comfortably high in terms of digital counts. Such waters being widely represented in the world ocean, the overestimate could be of importance, even if, at first sight, its amplitude does not appear to be dramatically high. It can be easily overcome by definitely replacing the empirical blue-to-green algorithm by the corresponding modelled algorithm.

A polynomial fit of the curves displayed in Figure 4 (RMS error less than 3 %) leads to the following expressions:

$$\log C = 0.347 - 2.73 (\log r_{1,3}) + 2.14 (\log r_{1,3})^2 - 2.04 (\log r_{1,3})^3 \quad \text{(IV } a\text{)}$$

(optimized for $C < 2$ mg.m^{-3})

$$\log C = 0.661 - 8.48(\log r_{2,3}) + 11.52 (\log r_{2,3})^2 - 88.38 (\log r_{2,3})^3 \quad \text{(IV } b\text{)}$$

(optimized for $C > 1$ mg.m^{-3})

Another advantage of using the above equations lies in their internal coherency. As discussed in the preceding section, above a certain pigment concentration threshold, with $L_w(443)$ and thus $r_{1,3}$ becoming unreliable, it is necessary to switch to an algorithm involving $r_{2,3}$. As shown by Figure 5, in the C range where the switching procedure must be operated (say around 1 or 2 mg.m^{-3}), the pigment estimates differ (by 10-15 %) according to whether the empirical algorithms involving $r_{1,3}$ or $r_{2,3}$ have been used. This discrepancy cancels out, and the continuity in the C estimate is, *a priori*, ensured if the compatible algorithms IV a and b are successively used (accordingly, $j = i = 1$ or 2, in Fig. 1 *a*).

SIMULATION OF OCEAN COLOUR REMOTE-SENSING (GENERAL SCHEME)

For purposes of studying the questions raised in the introductory analysis (extrapolation of aerosol properties, efficiency of the pixel-by-pixel procedure), it is more convenient to dispose of a simulated ocean-atmosphere system, than to use actual ocean colour data (in practice those provided by CZCS), where intricate influences of many parameters (oceanic and atmospheric, but also

radiometric) are beyond control. Within the frame of a model, these parameters can be easily mastered and sensitivity analyses can be effected without ambiguities. For another purpose, such an approach has already been adopted (André and Morel, 1989), and the general scheme previously developed for simulating the various remote sensing conditions is used for the following studies.

The ocean-atmosphere system described below is able to produce the total radiances $L_T(\lambda_i)$ that would be measured by CZCS in the four visible channels (i = 1 to 4), with given lighting and viewing conditions. These radiances can then be used as inputs when simulating the application of any CZCS data processing method. Thereafter the ocean and aerosol properties, once retrieved, can be compared to those initially introduced when generating the ocean-atmosphere system. This general scheme is displayed in Figure 6. The pigment concentration within the initial ocean is C, and the initial atmosphere contains an aerosol load F, with an aerosol Angström exponent, *n*; the corresponding retrieved values, C', F' and n', may (and generally do) differ from the initial values because, *a priori*, one or several assumptions on which the processing under scrutiny relies are not satisfied.

It is assumed that the marine and atmospheric contributions to the total radiances outside the atmosphere are separable quantities, therefore L_T can be computed according to equation 4 in Table 1. The signals contributing to L_T are modelled according to the steps set out below.

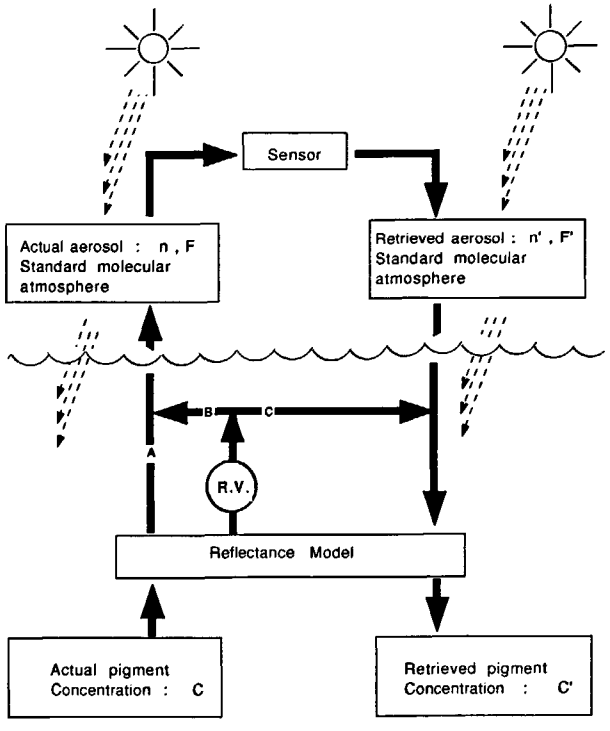

Figure 6

General scheme of the simulations. The black arrows follow the computation flow. R.V. : "Random Variations" (see text).
Schéma de principe des simulations. Les flèches noires suivent le sens du calcul. «R.V.» signifie «variations aléatoires» (*cf.* texte).

Marine signal: L_W

The optical model for Case 1 waters is used to compute the reflectances of the initial ocean as a function of its pigment content C, in the range 0.02 to 10 $mg.m^{-3}$. The initial ocean (in a first step) will strictly conform to the model (in the last part, this assumption will be relaxed, and a natural "noise" within the reflectance-pigment relationship will be considered). L_W is then computed through equation 14 (*see* Table 1), once given the transmittance of the atmosphere, and $F_o(\lambda)$, the extraterrestrial solar irradiance. The revised values used here for F_o are those of Neckel and Labs (1984), recently recommended by Gordon *et al.* (1988). The atmospheric diffuse transmittance, $t(\lambda,\theta)$, is computed according to equation 8. The presently selected values of the ozone and Rayleigh optical thicknesses correspond to a standard ozone content of 350 DU, and a standard barometric pressure of 1013.25 hPa.

Rayleigh signal: L_R

In BM this radiance was computed under the single scattering assumption (equation 5). However, according to Gordon and Castaño (1987), this assumption can no longer be considered as satisfactory. In the present paper L_R is computed according to Gordon *et al.* (1988), and includes multiple scattering and polarization effects. This improvement is symmetrically incorporated into the atmospheric correction procedures.

Aerosol signal: L_A

In the modelled atmosphere the radiances due to supposedly non-absorbing aerosols are computed according to equation 5' (with $\omega_A = 1$), where $p_A(\lambda,\theta,\theta_o)$ is expressed according to equation 7 (with $\gamma \pm$ from equation 7'). In addition, it is assumed that:

- the optical thickness $\tau_A(\lambda)$ varies with wavelength according to an Angström law:

$$\tau_A(\lambda) = \tau_A(\lambda o)\,(\lambda / \lambda_o)^n \qquad (V)$$

where the exponent n is assigned to be 0 or -1.

- the scattering varies with angle according to a two-term Heyniey-Greenstein phase function (like in Gordon and Castaño, 1987; André and Morel, 1989), expressed according to:

$$P_A(\gamma\pm) = f(\gamma\pm, g_1) + (1-\alpha)\, f(\gamma\pm, g\,2) \qquad (VI)$$

where; $f(\gamma, g) = (1- g) / (1+ g - 2g\cos\gamma)^{3/2}$,
and; $\alpha = 0.983$, $g_1 = 0.82$, $g_2 = -0.55$
In order to preserve the generality of the results, we avoid using absolute values of the aerosol phase function P_A, as it should be necessary if applying directly equation

5'. Instead, the aerosol radiance is scaled with respect to the Rayleigh radiance, thanks to an operational turbidity index, F, defined as being:

$$F = L_A (550\ nm) / L_R (550\ nm) \qquad (VII)$$

which is given the values 0.1 or 0.5. To fix the idea, with an aerosol exhibiting the above phase function, the corresponding τ_A (550 nm) values would be 0.058, and 0.29, respectively. L_A (550 nm) is determined as soon as an F value is decided. Changing of wavelength is effected through equation V, and changing of geometry through equation VI.

Among the possible combinations of the involved parameters, *i.e.* the aerosol load index F, the aerosol Angström exponent n, and the geometrical configuration, four representative situations have been selected (summarized in Tab. 2) as follows:

Table 2

Values of the aerosol Angström exponent n, of the aerosol load F and of the angles θ, θ_0 and φ (in degrees) for 4 selected remote sensing situations. The value F = 0.3 in situation 2 is such that the aerosol optical thickness is the same as in situations 1 and 3).
Valeurs de l'exposant d'Angström des aérosols n, de la charge en aérosol F et des angles θ, θ_0 et φ (en degrés), pour quatre situations choisies de télédétection. La valeur F = 0,3 dans la situation 2 conserve à l'épaisseur optique aérosol la même valeur que dans les situations 1 et 3).

set	n	F	θ	θ_0	φ
1	-1.0	0.5	30	0	90
2	-1.0	0.3	40	60	120
3	0.0	0.5	30	0	90
4	-1.0	0.1	30	0	90

• situation 1 is considered as a reference set; the atmosphere is moderately loaded by an aerosol with a spectral selectivity corresponding to n = -1 (a common value), and the constellation is favourable, in the sense that sun rays and sighting direction are not too far from nadir;
• situation 2 is designed separately to explore the influence of geometry alone upon the questions to be examined. Compared to 1, constellation 2 becomes unfavourable, to the extent that air masses are considerably increased, whereas the atmosphere properties are unchanged;
• situation 3 differs from the reference situation only in the nature of the aerosol, which now exhibits a non-selective scattering (n = 0);
• situation 4 differs from the reference situation only in the aerosol load, which is made typical of extremely clear atmospheres.

POSSIBLE PIGMENT MISESTIMATES RELATED TO THE USE OF A MEAN ANGSTRÖM EXPONENT

Before being averaged, the individual values obtained for the Angström exponent at the pixel scale (via BMP2) often show a rather wide dispersion. In BM, for instance, standard deviations of the order of 0.3 or even 0.5 around the mean n value are reported for Mediterranean or Mauritanian CZCS scenes. Part of this variability is due to the changing nature of aerosols. Another part,

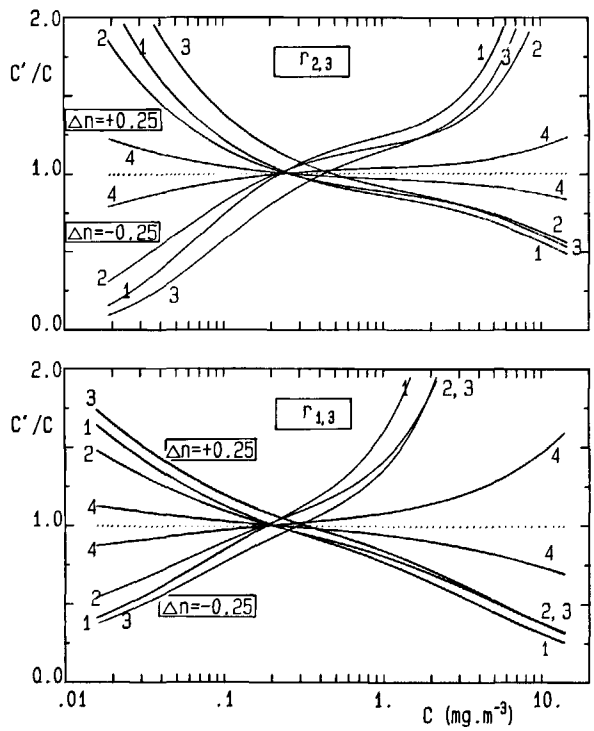

Figure 7

Ratio of the BMP1-estimated concentrations, C' (by following way A in Fig. 6), to the initial concentration, C, as a function of C, when the mean exponent differs from the actual value by Δ n = ±0.25, and for the four selected situations; the curves are numbered in reference to Table 2. Lower panel : BMP1 is based on the $r_{1,3}$ ratio. Upper panel: BMP1 is based on the $r_{2,3}$ ratio.
Rapport de la concentration C' évaluée par la procédure BMP1(en suivant la voie A de la fig. 6), à la concentration initiale C, en fonction de C, lorsque la valeur moyenne utilisée de l'exposant aérosol diffère de la valeur réelle par Δn = ±0.25. Les courbes sont numérotées en référence aux 4 situations choisies de la table 2. Panneau inférieur: la procédure BMP 1 repose sur le rapport $r_{1,3}$. Panneau supérieur: la procédure BMP 1 repose sur le rapport $r_{2,3}$.

however, is purely artefactual and results from a weakness within the processing method, which does not (and often cannot) account for all physical processes and all aspects of the radiative transfer involved. The aerosol phase function as well as their single scattering albedo are generally smooth functions of the wavelength, although this dependence is (necessarily) ignored in CZCS data processing. Gordon (1984) for instance found that this dependence leads, in the yet favourable case of a constant aerosol type, to variations in the ε (520,670) parameter along a scan line of the order of 0.05 (up to 0.09). The factor ε is related to n according to:

$$\varepsilon(\lambda,\lambda o) = (\lambda/\lambda_o)^{-n} \qquad \text{(VIII)}$$

When transcribed in terms of the Angström exponent, the above variations in ε correspond to variations in n, (= Δn), of 0.2 (up to 0.4). Gordon and Castaño (1987) predicted variations in ε within the same range, when this parameter is estimated in regions with different aerosol loads, due to the effect of the coupling between Rayleigh and aerosol scattering. This multiple and heterogeneous scattering term is neglected in the current CZCS data processing. André and Morel (1989) also found variations of the same order when the exponent is evaluated in regions with different ground pressures or ozone contents, as long as these differences are unknown and therefore neglected in the processing. Also, a wind-ruffled surface generates additional (and "neutral") signals at the spacecraft level, which are not separable from the aerosol effect, and thus influence the evaluation of n (see *e. g.* Tassan, 1981; Gordon, 1984). Consequently the local exponent values can significantly depart from their mean, even in presence of a uniform aerosol type within the examined area.

The impact of such departures upon the pigment concentration retrieval is investigated by simulating the application of the BMP1 (Fig. 1 *a*), to Case 1 modelled oceans, and by following way A in Figure 6. For that, n' (the mean value of the exponent presumably used in the processing), is forced to differ from the true value, n, by Δn; Δn could have been given any value within the range of expected possible departures (*see* above). For the sake of simplicity, only two discrete and plausible values are considered, say Δn = ± 0.25.

The results presented in Figure 7 show the variations of C'/C, *i.e.* the ratio of the retrieved-to-initial pigment concentration, as a function of the initial concentration, C, and for the four situations of Table 2. The lower panel is obtained when BMP1 is based on the $r_{1,3}$ ratio (iterative estimate of R (670) according to algorithm IIIa, and pigment estimate according to algorithm IVa), while the upper panel corresponds to the use of the $r_{2,3}$ ratio (algorithms III *b*, and IV *b*). As shown, a positive Δn leads to an over-estimate of the pigment concentration at low C-values, and conversely to an under-estimate of C in the high concentration range (the conclusions are reversed when Δn is negative). C remains well estimated if its value is around a hinge-point at about 0.1-0.3 $mg.m^{-3}$. Except perhaps for the very clear atmosphere of situation 4, the impact is never negligible. In moderately turbid atmospheres (situations 1 to 3), the procedure based on the $r_{1,3}$ ratio provides pigment estimates which can be erroneous by a factor 2 at very low concentrations (Fig. 7 *a*). The misestimates are even worst when C becomes higher than 2-3 $mg.m^{-3}$, but, as seen previously, the $r_{1,3}$ ratio should not be used in the high C-range. When BMP1 is based on the $r_{2,3}$ ratio, the misestimates would be largely heightened at low concentrations, but this ratio is not to be used for the low C-range. Inversely, and fortunately, the misestimates are significantly reduced in the high concentration range (Fig. 7 *b*). As shown, changing the geometry (curves 2 with respect to curves 1), or changing the initial exponent value (curves 3 with respect to curves 1) does not significantly modify the results. A by-product of the retrieval procedure is the aerosol load F'. Figure 8 presents the variations of the retrieved-to-initial load ratio F'/F, as a function of the initial concentration. In all the situations (and whatever the reflectance ratio used by the procedure), F' differs from F by only a few per cent, meaning that the aerosol load estimate is essentially unaffected by the inaccuracy in the Angström exponent. The effect of this inaccuracy is mostly suffered by the

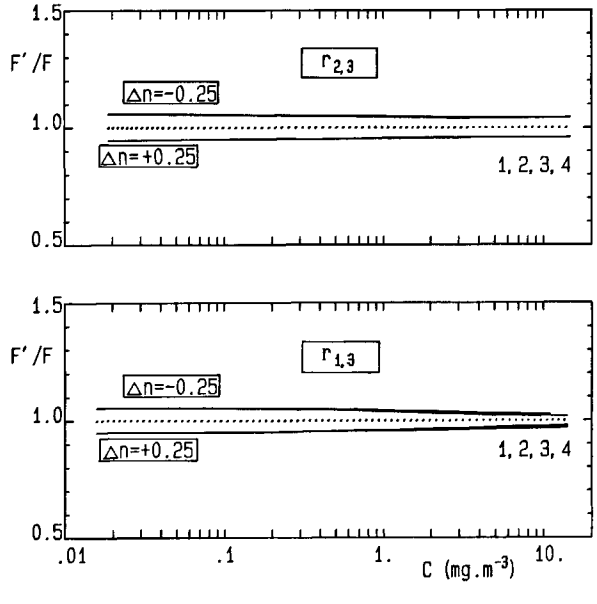

Figure 8

Ratio of the BMP1-estimated aerosol load, F', to the initial load, F, as a function of the pigment concentration C, and when the mean exponent differs from the actual value by Δ n = ±0.25, (and for the 4 situations). Lower panel: BMP1 is based on the $r_{1,3}$ ratio. Upper panel: BMP1 is based on the $r_{2,3}$ ratio.

Rapport de la charge en aérosol F', évaluée par la procédure BMP1, à la charge initiale F, en fonction de la concentration en pigments C, lorsque la valeur moyenne utilisée de l'exposant pour l'aérosol diffère de la valeur réelle par Δn = ±0.25, (pour les 4 situations choisies). Panneau inférieur: la procédure BMP 1 repose sur le rapport $r_{1,3}$; Panneau supérieur : la procédure BMP 1 repose sur le rapport $r_{2,3}$.

marine signal, and then by the pigment estimate.

THE PIXEL-BY-PIXEL PROCEDURE

Re-examination

This procedure, used as a trial by Bricaud and Morel (1987), produced the pigment content and aerosol maps of their Figures 6 and 15 *b*. These authors, however, expressed some reservations about an extensive use of such a method. A thorough re-examination of its practical efficiency is thus called for. With this aim, the application of the PPP to Case 1 modelled ocean is simulated, again by following way A in Figure 6. Under these conditions, all the hypotheses on which the PPP relies are verified (in particular, the ocean strictly obeys the optical model which is the core of the procedure). The three quantities simultaneously retrieved, *i.e.* the aerosol exponent, the aerosol load, and the pigment concentration, should therefore coincide perfectly with the initial values, if the PPP works well.

As regards pigment concentration, the results of the simulations, presented in Figure 9, partly contradict these expectations. The lower panel is obtained when the PPP is based on the $r_{1,3}$ ratio, as was the case in BM. In all the situations of Table 2, C' perfectly coincides with C, provided that C is less than about 2 mg.m^{-3}. Above this limit value, C' appears to diverge progressively from the initial value and the effect becomes dramatic at high concentration (with a variable amplitude according to the situation envisaged). The same general trends are observed for the retrieved exponent and load (lower panel in Fig 10 and 11, respectively).

The sign and magnitude of these biases (in C', F', and n'), which occur above 2 mg.m^{-3}, are not immutable. The results in Figures 9, 10 and 11 have been obtained by assigning the value 0 to the aerosol exponent at the entry of the iterative process (Fig. 1 *c*). If, for instance, the exponent had been given, as an initial first guess, a value higher than the actual value, the PPP would have led, for C > 2 mg.m^{-3}, to successive increasing overestimates of the three parameters, in such a way that the convergence could never have been achieved. An exhaustive presentation of such results for all the possible cases is useless. The essential fact is that the PPP, operated with $r_{1,3}$, is inherently unable to perform both the atmospheric correction and the pigment retrieval, when C is more than about 2 mg.m^{-3}. The origin of this unexpected failure in the PPP is basically linked to the evolution of the marine reflectances in the different CZCS channels with increasing pigment concentration (Fig. 1, in BM). When C increases, R (443) is always monotonously decreasing, whereas R (550), after a maximum, decreases and parallels R (443), when C > 1.8 mg.m^{-3}. In this C-range, such parallelism prevents the iterative procedure from being stable and reliable. Numerical experiments have confirmed this explanation.
Among the possible consequences, the phytoplankton concentration and aerosol maps may present a strong correlation in regions with high concentrations (as actually observed; Fig. 6 and 15 *b* in BM).

In spite of this limitation, the excellent agreement between C and C' in a wide range of concentration (say 0.015 to 1.5 mg.m^{-3}) constitutes a strong argument in favour of using the pixel-by-pixel procedure, since its failure occurs approximately at the same C value for which $L_W(443)$ in any case becomes unreliable (note that this statement is to be revised with an improved, more sensitive colour sensor). With CZCS, the blue-to-green reflectance ratio being abandoned and replaced by the blue-green-to-green ratio for the retrieval of concentrations higher than, say, 1.5 mg.m^{-3}, it remains to be determined whether the PPP, switched to the $r_{2,3}$ ratio, behaves well in this high concentration range.

The results of a simulation as above, but using $r_{2,3}$, are presented in the upper panels of Figures 9, 10 and 11 for the full C range, even if, in practice, the $r_{2,3}$ ratio has not to be used at low concentration. As shown, the PPP allows a perfect retrieval of the three parameters (in the ideal conditions of this simulation), for pigment concentrations as high as 10 mg.m^{-3}. Above this value, the procedure is again in check, with retrieved values diverging from the initial ones (this failure is also related to the manner the modelled reflectances vary with C, at high C-values).

If the switching capability (effected at 1-1.5 mg.m^{-3}), is included in the PPP (this is consistent with the magnitude of the marine signals as measured by CZCS), this procedure appears to be reliable over the (almost) entire range of pigment concentrations.

Response to the natural variability of marine optical properties

The reflectance model on which the procedures under study are based is representative only in average of the natural properties of Case 1 waters. For a given value of C, observed reflectances spread around the mean value predicted by the model (Fig. 1 in BM), mainly as a consequence of variations in the absorption and scattering properties of phytoplankton algae, and also in the relative proportions of algal and non-algal materials. This variability, inevitably ignored when processing satellite visible data, is expected to have some effects upon the satellite-derived products. With a processing method such as the PPP, these products concern both the atmosphere (aerosol properties) and the ocean (pigment content).
These effects are simulated in this section by allowing the reflectances at the surface of the initial ocean to

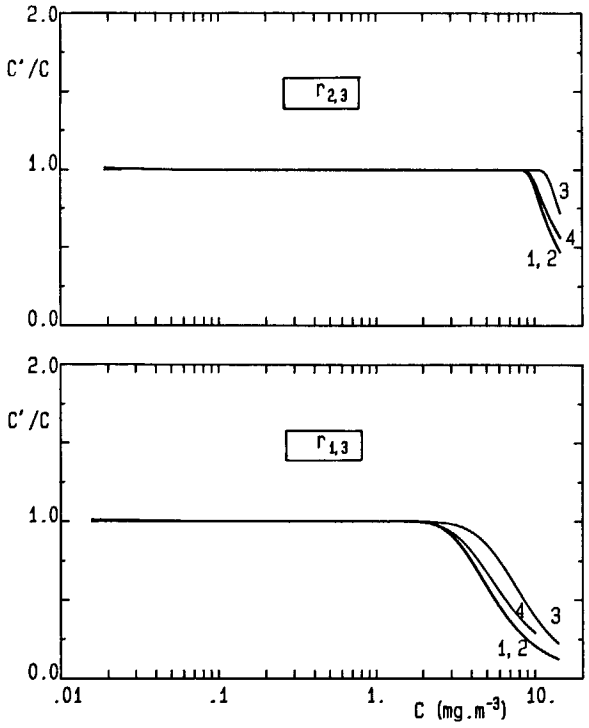

Figure 9

Ratio of the PPP-estimated pigment concentration, C' (by following way A in Fig. 6) to the initial concentration, C, as a function of C, and for the four selected situations. PPP is operated with the $r_{1,3}$ ratio and with the $r_{2,3}$ ratio in the lower and upper panels, respectively.
Rapport de la concentration en pigments C' évaluée par la procédure PPP (en suivant la voie A de la Figure 6), à la concentration initiale C, en fonction de C, pour les quatre situations choisies. Panneau inférieur: la procédure PPP repose sur le rapport $r_{1,3}$; Panneau supérieur: la procédure PPP repose sur le rapport $r_{2,3}$.

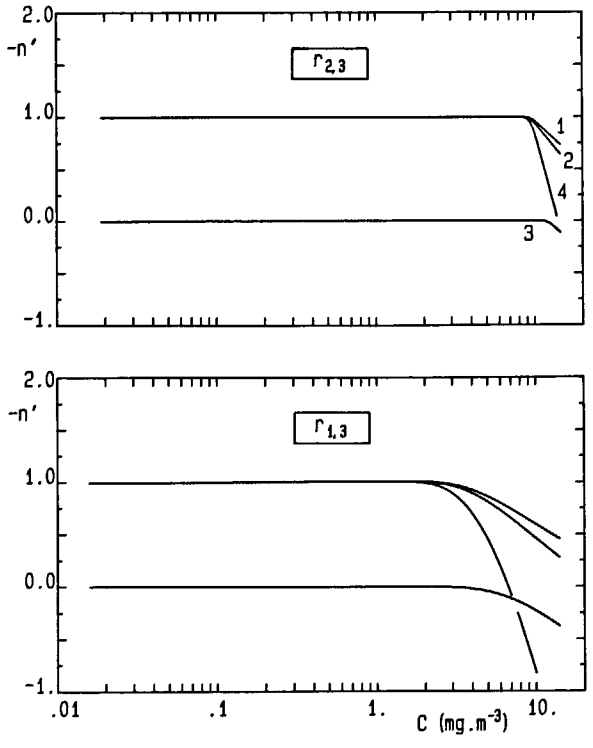

Figure 10

PPP-estimated aerosol exponent, n' (by following way A in Fig. 6), as a function of initial pigment concentration, C, and for the four selected situations. Lower panel: PPP is based on the $r_{1,3}$ ratio. Upper panel: PPP is based on the $r_{2,3}$ ratio.
Exposant aérosol n', évalué par la procédure PPP (en suivant la voie A de la fig. 6), en fonction de C, pour les quatre situations choisies. Panneau inférieur : la procédure PPP repose sur le rapport $r_{1,3}$. Panneau

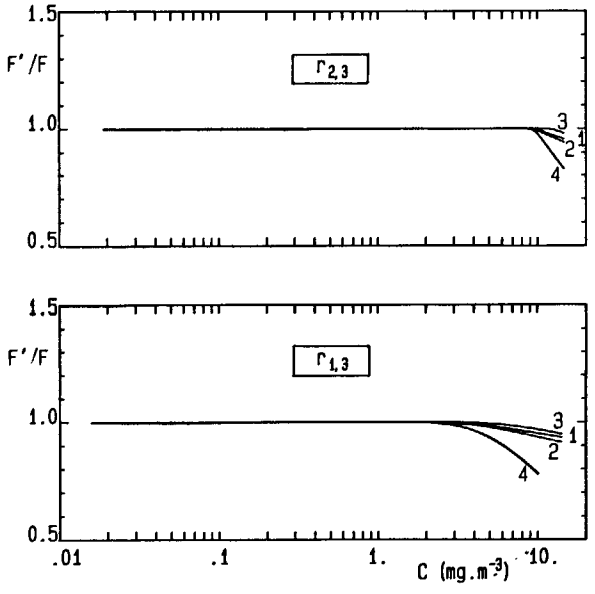

Figure 11

Ratio of the PPP-estimated aerosol load, F' (following way A in Fig. 6), to the initial load, F, as a function of the initial pigment concentration, C, and for the four selected situations. Lower panel: PPP is based on the $r_{1,3}$ ratio. Upper panel: PPP is based on the $r_{2,3}$ ratio.
Rapport de la charge aérosol F', évaluée par la procédure PPP (en suivant la voie A de la fig. 6), à la charge initiale F, en fonction de C, pour les quatre situations choisies. Panneau inférieur : la procédure PPP repose sur le rapport $r_{1,3}$. Panneau supérieur : la procédure PPP repose sur le

fluctuate randomly around the Case 1 modelled values. Note that systematic deviations may also exist, for instance in the presence of coccoliths (Gordon *et al.*, 1988). For each value given to the initial concentration (75 discrete C values in the range 0.02 to 10 $mg.m^{-3}$), 500 sets of "noisy" reflectances values, $R^*(\lambda)$, in CZCS channels 1 to 4, were generated around the modelled values, $R_m(\lambda)$, according to:

$$R^*(\lambda) = \{1 + |f| [A(C)]\}^s \{1 + |f'_\lambda| B_\lambda\}^{s'} R_m(\lambda) \quad (IX)$$

The first bracketed term modifies the reflectance levels for the whole spectrum, whereas the second term introduces a decorrelation between the channels.
More explicitly:
- f and f'_λ are independent ramdom numbers obeying Gaussian probability distributions (with 99 % of their values between +1 and -1). One value for f is generated for each reflectance set (*i.e.* each spectrum), and one value for f'_λ is generated for each of the four wavelengths within each spectrum;
- s is equal to +1 (resp. -1), when f is positive (resp. negative), and s' is equal to +1 (resp. -1), when f'_λ is positive (resp. negative);
- A (C) is an amplitude, directly proportional to log (C). This dependency accounts for the fact that, in the natural environment, blue waters are less fluctuating with respect to the model than chlorophyll-rich green waters.
- B_λ is an amplitude, assumed to be directly proportional to the relative spectral distance between the channels, *i.e.* to $|\lambda - 550| / 550$.

At the 99 % probability level (3σ), these noisy reflectance spectra differ in magnitude from the Case 1 model spectrum by up to ± 10 % when C is 0.02 $mg.m^{-3}$, and by up to ± 40 % when C is 10 $mg.m^{-3}$, and simultaneously for all channels. The decorrelation between the reflectances in channels 1, 2 and 4, with respect to that in channel 3, are respectively distributed (with a probability of 99 %, 3σ), between ± 12 %, ± 6 %, and ± 11 %.

A direct action on the marine reflectances has been preferred to operations at the level of the optical properties which govern reflectance (essentially the back scattering coefficient b_b, of phytoplankton and associated detritus plus seawater, and their absorption coefficient, a, through the ratio b_b/a). Care has been taken, however, to ensure realistic fluctuations in terms of absorption and scattering by phytoplankton. In the bio-optical models of Morel (1988) and of Gordon *et al.*, (1988), this scattering is expressed through a coefficient, b (550), which varies with chlorophyll according to $b(550) = b_o C^{0.62}$. The fluctuations imposed in the magnitude of the reflectance spectra would then correspond to random variations of the order of ± 40 % in b_o (a factor which may vary by ± 50 % around a mean value of 0.3; *see* in Gordon and Morel, 1983). As regards the decorrelation between the reflectance values in the four channels, they are consistent with the possible variations in absorption properties of algal populations (examples of inter-species variations can be found, *e.g.* in Bricaud *et al.*, 1988).
In order to understand how the PPP can cope with such reflectance spectra, the prerequisite is to examine the disturbance affecting the pigment estimate that is only due to the superimposed noise, and outside any atmospheric interference. For that, the pigment algorithms (IV *a* if C < 1 $mg.m^{-3}$, and IV *b* otherwise), are directly applied to the fluctuating marine reflectances (way C in Fig. 6). Note that such an application simulates an ideal situation (to be approached, it may be hoped, by future sensors), in which the atmospheric signals would be accurately assessed.

In comparison with the initial values, Figure 12 shows some examples of the pigment estimates derived from the randomly fluctuating reflectances (10 C' values among the 500 computed for each of the 75 discrete C values). For each initial C value, the 500 C'/C ratios are averaged, and the standard deviations around the means are computed. Figure 13 *a* shows the mean ratios (dotted line) ± 1 standard deviation (solid curves). In average, C'/C = 1 everywhere within the considered C range, and the standard deviation is at the most ± 25 % at both ends of the range. Such a magnitude for the dispersion compares well with the 30-35 % standard deviation errors typical of empirical pigment algorithms (Gordon *et al.*, 1983). This suggests that the fluctuations of the marine reflectances considered in the present sensitivity study are reasonable. The dispersion obviously originates only from the decorrelated fluctuations introduced in channels 1, 2 and 3 since the algorithms which depend on the use of the $r_{1,3}$ or $r_{2,3}$ ratios are, by nature, insensitive to

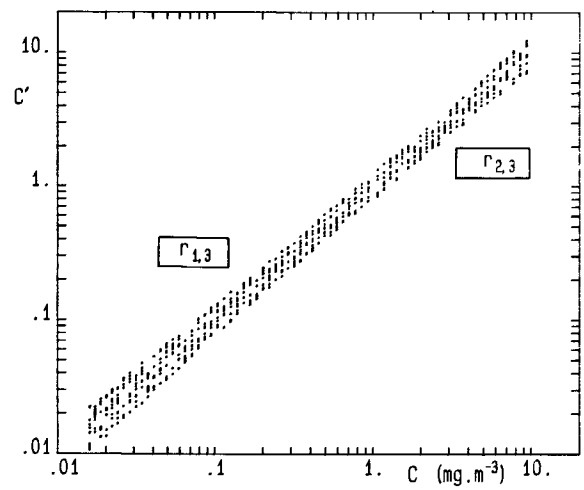

Figure 12

When the $r_{1,3}$ or $r_{2,3}$ -pigment algorithms are applied to the noisy reflectances (by following way C in Fig. 6, with no atmosphere) the retrieved concentrations, C', differ from the initial values C, as shown by plotting C' as a function of C. For each of the 71 discrete C values, 500 C' estimates were obtained; only ten selected at random are shown.
Lorsque les algorithmes pigments basés sur les rapports $r_{1,3}$ et $r_{2,3}$ sont appliqués aux réflectances «bruitées» (en suivant la voie C de la fig. 6, *i.e.* en l'absence d'atmosphère), les concentrations calculées C' diffèrent des valeurs initiales C, comme il apparaît en reportant C' en fonction de C. Pour chacune des 71 valeurs discrètes de C, 500 estimations de C' ont été obtenues, parmi lesquelles dix valeurs seulement (choisies au hasard) sont montrées.

the absolute values of the various R (λ) and to their variations, provided that they remain proportional.
This statement does not hold true as soon as the atmospheric correction (which involves the absolute radiance values) is effected. Thus the manner in which the PPP responds to the ocean fluctuations is simulated by using the same set of noisy reflectances (way B in Fig. 6), and the results are displayed in Figures 13 *b*, *c* and *d*.
For concentrations less than 1 $mg.m^{-3}$, the PPP is operated with the $r_{1,3}$ ratio; and otherwise, with the $r_{2,3}$ ratio.

As regards the pigment estimate (Fig. 13 *b*), the averaged C' values coincide (dotted line) with the initial C values, as far as C < 2 or 3 $mg.m^{-3}$. For higher initial concentrations, the averaged C'/C ratios are lower than 1, with a difference which depends upon the remote sensing conditions. The origin of this trend is understandable; part of the randomly generated spectra in the range of high C cannot be processed because the PPP identifies negative $L_W(520)$ values at some stage of the iterative computation, and therefore stops. If, conversely, the random noise results in an enhancement of this signal, the procedure can work and produces a C' value below C. On average, the C' values are therefore lower than C (this dissymmetrical response of the PPP to the natural noise has to be kept in mind when the PPP is operated for CZCS scenes, without precluding its application). Considering the whole concentration range, the standard deviation around the mean is now between ± 20 % (for the lowest C values) and ± 50 % (for C > 3 $mg.m^{-3}$), and is restrained to ± 25 % for most of the waters. These last figures are hardly above those displayed in Figure 13 *a*. The encouraging conclusion is that, as regards the question of marine optical variability, the quality of the pigment estimate, as attainable with the PPP (*i.e.* including the atmospheric correction), is comparable to the (limiting) capability of the sole pigment algorithms.

Because the estimate of the aerosol parameters is deeply imbricate, inside the PPP, with the pigment estimate, these parameters are also expected to undergo some defects owing to the ignored marine optical variability. As regards the aerosol exponent retrieval, the results are presented in Figure 13 *c*. The mean n' values coincide

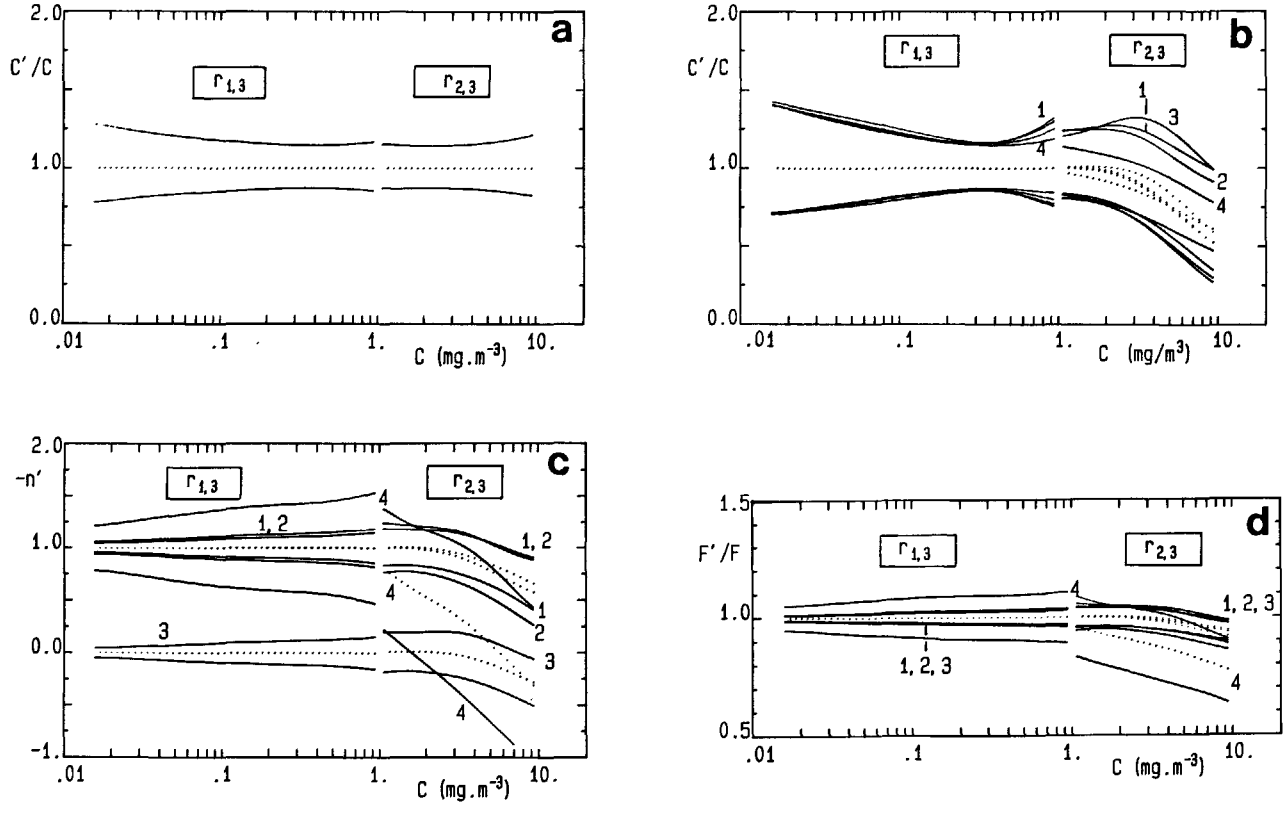

Figure 13

a) *As for Figure 12, except that the 500 C'/C ratios obtained for each initial C value were averaged and are plotted (dotted line) as a function of C. The solid lines correspond to ± one standard deviation around the average.*
b) *Ratio of the PPP-estimated concentration C' (following way B in Fig. 6), to the initial value, C, as a function of C, for the four selected situations. Dotted line : averaged values. Solid lines correspond to ± one standard deviation from the average. PPP makes use of the $r_{1,3}$ ratio when C is less than 1 $mg.m^{-3}$, and of the $r_{2,3}$ ratio when C is higher.*
c) *Same as in Figure 13 b, but for the PPP-estimated aerosol exponent, n'.*
d) *Same as in Figure 13 b, but for the ratio of the PPP-estimated aerosol load, F', to the initial value, F.*
a) Comme pour la Figure 12, à ceci près que les 500 rapports C'/C obtenus pour chaque valeur de la concentration initiale C ont été moyennés et sont portés (droite en pointillé) en fonction de C. Les courbes en trait continus correspondent à ± l'écart type autour de la moyenne.
b) Rapport de la concentration C' évaluée par la procédure PPP (en suivant la voie B de la fig. 6), à la valeur initiale C, en fonction de C pour les 4 situations choisies. Trait pointillé : valeurs moyennes. Les traits continus correspondent à ± l'écart type autour de la moyenne. La procédure repose sur le rapport $r_{1,3}$ lorsque C est inférieur à 1 $mg.m^{-3}$ et sur le rapport $r_{2,3}$ dans le cas contraire.
c) Comme pour la figure 13 *b*, mais pour l'exposant aérosol n', évalué par la procédure PPP.
d) Comme pour la figure 13 *b*, mais pour le rapport de la charge aérosol F', évaluée par la PPP, à la charge initiale F.

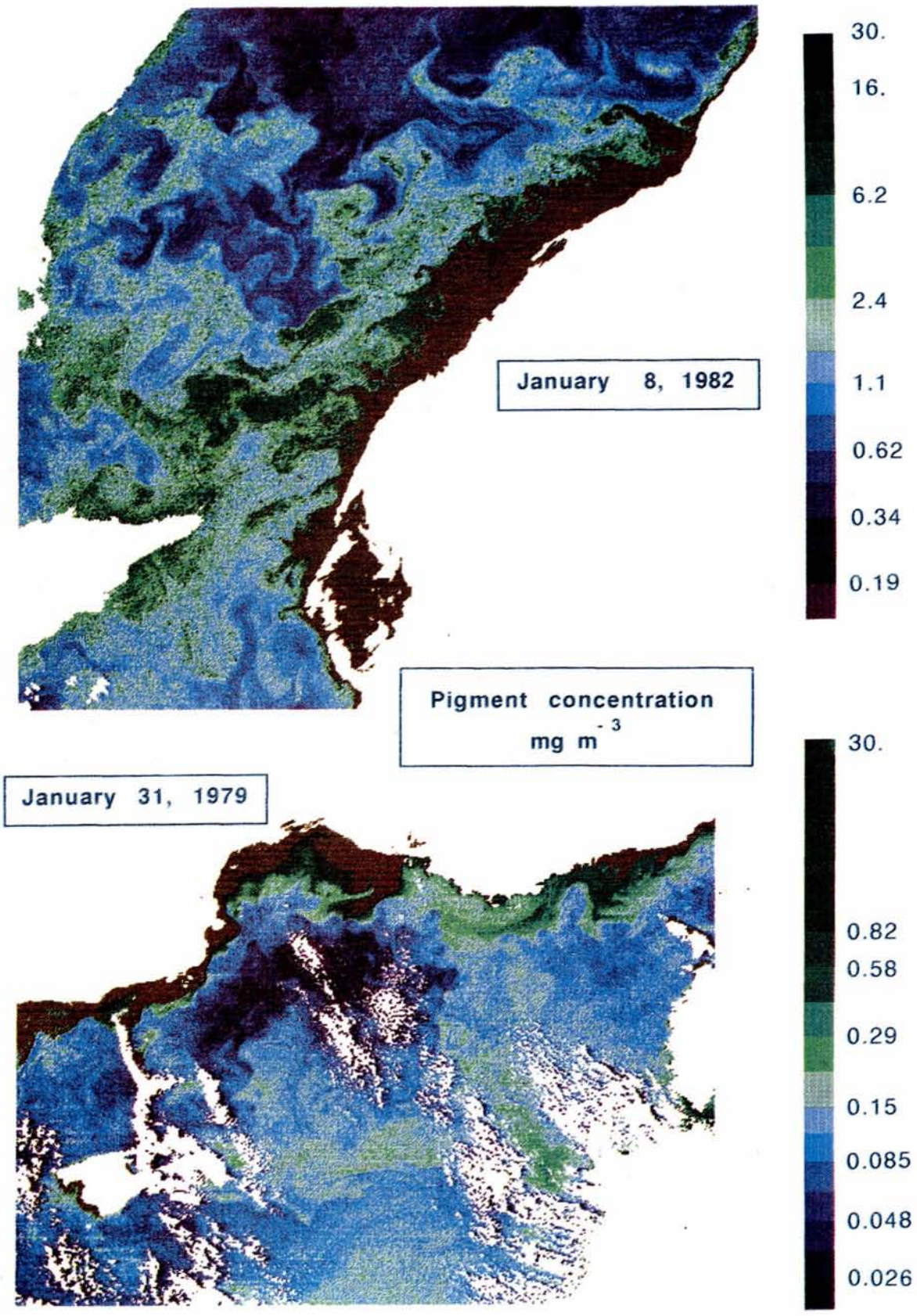

Figure 14

Phytoplankton pigment distributions produced through the application of the modified procedure (PPP based on the $r_{1,3}$ and $r_{2,3}$ modelled algorithms) to a CZCS scene (8 January, 1982) of the Mauritanian coastal upwelling (upper panel), and to a (31 January, 1979) scene of the Northwest Mediterranean (lower panel). Lands and clouds are flagged in white, and (turbid) Case 2 waters in brown.

Distribution spatiale des pigments phytoplanctoniques obtenue en appliquant la procédure modifiée (la PPP utilisant les algorithmes modélisés basés sur les rapports $r_{1,3}$ et $r_{2,3}$), à une scène CZCS (8 Janvier 1982) de l'upwelling Mauritanien (image du haut), ainsi qu'à une scène (31 Janvier 1979) de la Méditerranée Nord-Occidentale (image du bas). Les terres et les nuages sont masqués en blanc et les eaux du cas 2 (turbides) en brun.

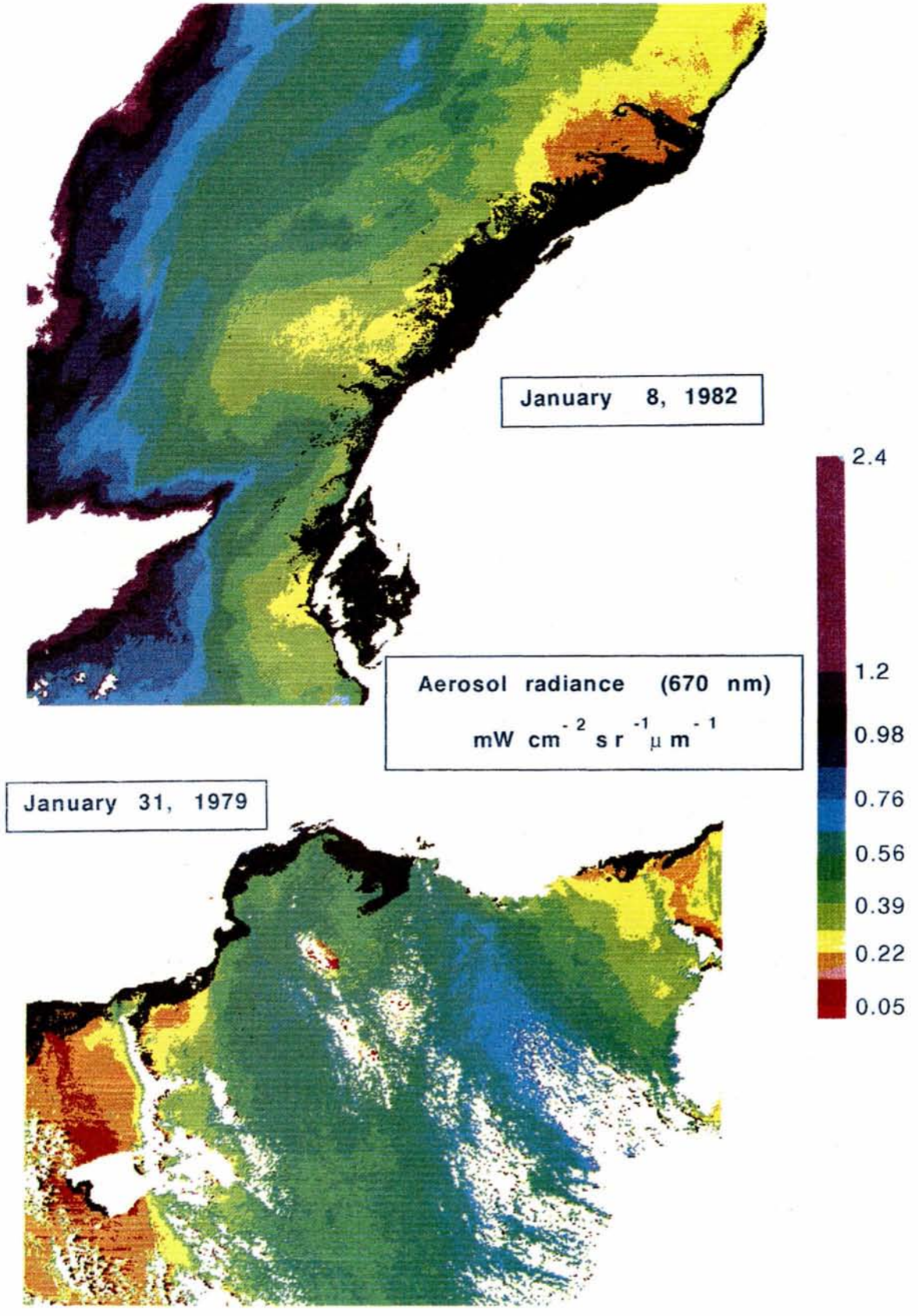

Figure 17

Aerosol radiance (at 670 nm) distributions in correspondence to the pigment distributions in Figure 14. Black pixels correspond to Case 2 waters.
Distributions de la luminance aérosol (à 670 nm) correspondant aux distributions en pigments de la Figure 14. Les pixels en noir marquent les eaux du cas 2.

with the initial n value, except if C is more than 2-3 $mg.m^{-3}$. In terms of standard deviation, the departure of n' from n is in the range 0.05-0.2 for situations 1,2 and 3; it becomes considerably higher (0.25 to 0.5) in the clear atmosphere of situation 4, for which the weaker aerosol signals are more affected. For the aerosol load retrieval (Fig. 13 *d*), the trends are similar to those found for the exponent retrieval, with a standard error of estimate of the order of only a few per cent in most cases, except in the unfavourable case of reduced aerosol load (situation 4). As expected, a major part of the noise in the natural pigments-to-reflectance relationship is "transferred" to the retrieved aerosol parameters, particularly to the Angström exponent, and for this reason, the pigment assessment through the PPP remains not only possible, but also sufficiently accurate.

PRACTICAL CONSEQUENCES OF THE PROPOSED MODIFICATIONS

With respect to the currently available methods developed for CZCS data processing, some modifications have been proposed. They consist in an extensive use of the pixel-by-pixel procedure and also in the use of a coherent set of relationships (linking reflectance ratios to reflectance ratios and to pigment concentration), all derived from the same bio-optical model. These modifications, logically believed to be improvements, are based upon rational arguments. Nonetheless, it cannot be irrefutably claimed that more accurate pigment determinations are reached via this improved method. Only a series of sea-truth measurements over a long period and wide areas could bring the final proof. It is therefore worth examining whether processed CZCS scenes differ significantly when the proposed method replaces the previous one. Thus, in order to examine the practical consequences of operating the PPP instead of the BM "mean exponent" procedure, and of using modelled rather than empirical algorithms, two CZCS scenes, acquired with "normally" clear atmospheres, have been selected, as encompassing very distinct pigment concentration ranges.

The processing of the 8 January, 1982 scene copes with the high concentrations typical of the Mauritanian upwelling (Fig. 14, upper pannel). This image was produced using the PPP (the modelled relationships III *a*, *b* and IV *a*, *b* are used, and the switch from the $r_{1,3}$ ratio to the $r_{2,3}$ ratio is operated for concentrations greater than 1 $mg.m^{-3}$). Curve 1 in Figure 15 *a* shows the pigment histogram corresponding to the image in Figure 14 and curve 2 corresponds to the application of the BM procedure (with a computed mean value of the Angström exponent equal to 0.4, combined with empirical algorithms). As shown, the two frequency distributions diverge slightly; the BM procedure produces more numerous pixels with concentrations in the range 1-3 $mg.m^{-3}$ and relatively fewer pixels with high concentrations. In addition, the $r_{1,3}$-to-$r_{2,3}$ switch in the BM procedure introduces a noticeable discontinuity in the histogram which does not occur with the PPP. In Figure 15 *b*, curve 1 corresponds to the PPP based only on the modelled $r_{1,3}$ algorithms and curve 2 corresponds to the PPP based on the $r_{1,3}$ empirical algorithms. It is worth noting that the replacement of modelled by empirical algorithms results in a translation of the histogram towards higher concentrations (note, however, that the PPP depending only on the $r_{1,3}$ ratio should not be used at high concentrations). To the extent that the modelled algorithms are believed to provide a more realistic description of marine optical properties, the empirical algorithms, in comparison, lead to an

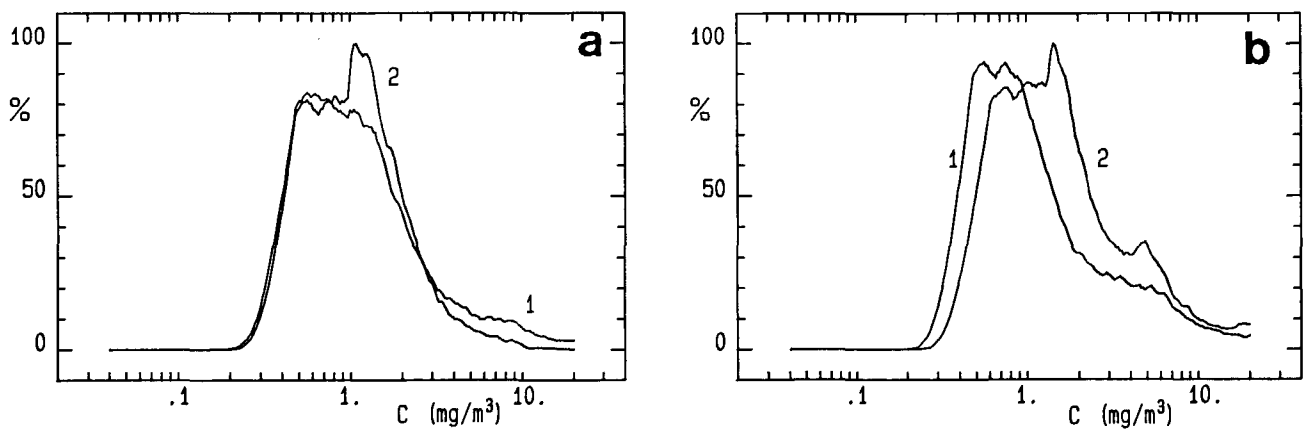

Figure 15

Pigment concentration histograms obtained when applying various procedures to the Mauritanian scene.
a: Curve 1; PPP based on the $r_{1,3}$ and $r_{2,3}$ modelled algorithms. Curve 2; BM procedure (empirical algorithms and use of a mean exponent).
b: Curve 1 ; PPP based on the $r_{1,3}$ modelled algorithms. Curve 2; PPP based on the $r_{1,3}$ empirical algorithms.
Histogrammes des concentrations en pigments obtenus en appliquant diverses procédures à la scène Mauritanienne.
a : Courbe 1 : PPP utilisant les algorithmes modélisés basés sur les rapports $r_{1,3}$ et $r_{2,3}$. Courbe 2 ; procédure BM (algorithmes empiriques et usage d'un exposant aérosol moyen).
b : Courbe 1 : PPP utilisant les algorithmes modélisés basés sur le rapport $r_{1,3}$. Courbe 2 ; PPP utilisant les algorithmes empiriques basés sur le rapport $r_{1,3}$.

overestimate of the pigment concentration.
The processing of the 31 January, 1979 scene copes with the very low concentrations remaining in the area of winter intense vertical mixing leading to dense water formation, in the northern part of the Mediterranean Sea (Fig. 14, lower panel). This image was produced by operating the PPP based only on the algorithms involving the $r_{1,3}$ ratio, since high concentrations are not represented in this zone. Curve 1 in Figure 16a shows the pigment histogram corresponding to this processing, and curve 2 corresponds to the application of the BM procedure (with a mean computed value of the Angström exponent of 0.8). The use of a mean exponent turns out to be inadequate for the processing when dealing with such low pigment concentrations. In effect, the total number of pixels which can be processed with the BM procedure (curve 2) is significantly lower than with the PPP. In Figure 16 *b*, curve 1 is redrawn from Figure 16 *a*, while curve 2 corresponds also to the PPP, when based on the $r_{1,3}$ empirical algorithms. As previously pointed out (Fig. 15 *b*), the use of the empirical instead of the modelled algorithms provokes a translation of the histogram towards higher concentrations, and a general overestimate.

For each Case 1 water pixel, the PPP provides simultaneous estimates of the pigment concentration and of the aerosol parameters. From several (already quoted) studies, and as emphasized in the present one, the CZCS Angström exponent estimate is known to suffer severely from departure with respect to the inescapable assumptions adopted in the processing, with the consequence that the Angström exponent value is the most questionable retrieved parameter. In most cases, it should not be considered as a reliable by-product of CZCS pigment retrieval.

On the other hand, confidence can reasonably be placed in the estimate of the aerosol radiance at one wavelength: at 550 nm and, better, at 670 nm, where the marine contribution to the remotely-sensed radiance is always particularly small (for Case 1 waters). As an example, Figure 17 shows the distributions of L_A (670) in correspondence with the pigment maps of Figure 14. The aerosol radiances are well organized in atmospheric-like structures, with the highest values aligned in the vicinity of the clouds. The decoupling between pigment and atmospheric features is indubitably achieved, as clearly demonstrated by comparing the patterns in Figures 14 and 17. According to Gordon and Castaño (1989), these radiances could be corrected for aerosol multiple scattering and interaction between Rayleigh and aerosol scattering. This would permit a precise (and simple) transcription of the CZCS aerosol radiances into optical depth, to the extent that a representative scattering phase function could be attributed to the aerosol population.

CONCLUSION

After having identified and analysed several sources of uncertainties or shortcomings inherent in the available methods, previously developed for the CZCS data processing, some modifications are proposed, as summarized in the following concluding remarks.

• Modelled relationships can be reliably used and are preferred to empirical relationships, which, due to their statistical and noisy nature, cannot ensure a full internal consistency. With these modelled relationships, the marine reflectances and their two-by-two ratios are inter related or are related to the pigment concentration within a coherent frame. Besides this conceptual improvement, a practical advantage lies in the fact that the blue channel can be replaced by the blue-green channel when necessary without *a priori* numerical mismatch. The rather poor sensitivity of the 520/550 reflectance ratio

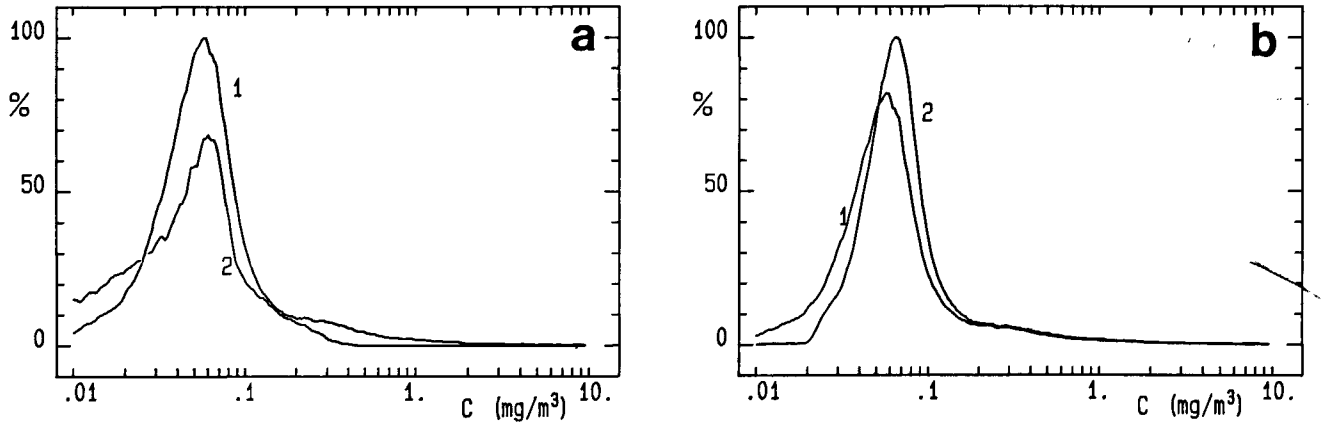

Figure 16

Same as in Figure 15, but for the Mediterranean scene, and except that the $r_{2,3}$ algorithms are not used.
Comme pour la Figure 15, mais pour la scène Méditerranéenne, et à la différence que les algorithmes basés sur le rapport $r_{2,3}$ ne sont pas employés.

regarding the pigment assessment is acknowledged. At least for CZCS data, the recourse to this ratio, however, remains of order when dealing with high pigment concentrations;

• Natural (or artifactual) variations in the Angström exponent cannot be ignored and the use of a mean value for this exponent must be avoided as far as possible (over Case 1 waters). Therefore the pixel-by-pixel procedure, which does not require such an averaging, is recommended. The individual values produced for this exponent (at the pixel scale) are known to be deeply affected by the various assumptions on which the processing relies; in particular, they are influenced by the fluctuating differences which may exist between the actual optical properties of the ocean and those set by the reflectance model. Consequently, the retrieved exponent values can hardly be considered as a reliable by-product;

• Counterbalancing this weakness, the pigment concentrations appear to be safely assessed in spite of the possible deviations with respect to the model (these deviations are partially "re-incorporated" into the atmospheric correction, and distort the Angström exponent values);

• The aerosol optical thickness as estimated in the 670 nm spectral band can be derived with an acceptable accuracy, at least over low-chlorophyll clear waters, *i.e.* for the greater part of the ocean.

Acknowledgements

The support of the *Centre National de la Recherche Scientifique* (under contract UA 353) and of the *Centre National d'Etudes Spatiales* (88/1285) are duly acknowledged. We also express particular appreciation to Annick Bricaud and to Howard Gordon for their help and criticisms. This work is a contribution to the research encouraged by the IAPSO commission "Oceanography from Space".

REFERENCES

André J.-M., A. Morel (1989). Simulated effects of barometric pressure and ozone content upon the estimate of marine phytoplankton from space. *J. Geophys. Res.*, **94**, 1029-1037.

Bricaud A., A. Morel (1987). Atmospheric corrections and interpretation of marine radiances in CZCS imagery: use of a reflectance model. *Oceanol. Acta*, **7**, 33-50.

Bricaud A., A.L. Bédhomme, A. Morel (1988). Optical properties of diverse phytoplanktonic species: experimental results and theoretical interpretation. *J. Plankton Res.*, **10**, 851-873.

Gordon H.R., J. Brown, R.H. Evans (1988). Exact Rayleigh calculations for use with the Nimbus 7 Coastal Zone Color Scanner. *Appl. Opt.*, **27**, 862-871.

Gordon H.R., O.B. Brown, R.H. Evans, D.K. Clark (1983). Nimbus 7 CZCS: reduction of its radiometric sensitivity with time. *Appl. Opt.*, **22**, 3929-3931.

Gordon H.R., O.B. Brown, R.H. Evans, J.W. Brown, R.C. Smith, K.J. Baker, D.K. Clark (1988). A semianalytic model of ocean color. *J. Geophys. Res.*, **93**, 10909-10924.

Gordon H.R., D.J. Castaño (1987). Coastal Zone Color Scanner atmospheric algorithm: multiple scattering effects. *Appl. Opt.*, **26**, 2111-2122.

Gordon H.R., D.J. Castaño (1989). Aerosol analysis with the Coastal Zone Color Scanner: a simple method for including multiple scattering effects. *Appl. Opt.*, **28**, 1320-1326.

Gordon H.R., D.K. Clark (1981). Clear water radiances for atmospheric correction of Coastal Zone Color Scanner imagery. *Appl. Opt.*, **20**, 4175-4179.

Gordon H.R., D.K. Clark, O.B. Brown, R.H. Evans (1982). Satellite measurement of phytoplankton pigment concentration in the surface waters of a warm core Gulf Stream ring. *J. Mar. Res.*, **40**, 491-502.

Gordon H.R., D.K. Clark, J.W. Brown, R.H. Evans, W.W. Broenkow (1983). Phytoplankton pigment concentrations in the Middle Atlantic Bight: comparison of ship determinations and CZCS estimates. *Appl. Opt.*, **22**, 20-36.

Gordon H.R., A. Morel (1983). Remote assesment of ocean color for interpretation of satellite visible imagery: a review, in: Lecture Notes on Coastal and Estuarine studies, ed. by M. Bowman, Springer-Verlag, 114 pp.

Morel A. (1983). Optical modelling of the upper ocean attenuance and reflectance in relation to biogenous material content ("Case 1" waters). Ass. IUGG/IAPSO, Hamburg, Abstract vol. PS7, 148-149.

Morel A. (1988). Optical modelling of the upper ocean in relation to its biogenous matter content (Case 1 waters). *J. Geophys. Res.*, **93**, 10747-10768.

Neckel H., D. Labs (1984.) the Solar radiation between 3 300 and the 12 500 A. *Solar Physics*, **90**, 205-258.

Smith R.C., W.H. Wilson (1981). Ship and satellite bio-optical research in the California Bight, in: Oceanography from Space, ed. by J.F.R. Gower, Plenum Press, New-York, 281-294.

Tassan S. (1981). The influence of wind in the remote sensing of chlorophyll, in: Oceanography from Space, ed. by J.F.R. Gower, Plenum Press, New-York, 371-375.